



**DETERMINATION OF FATIGUE STRESS OF
ACCELERATED COOLED S275 QUALITY
PROFILE STEELS**

**2024
MASTER THESIS
METALLURGICAL AND MATERIALS
ENGINEERING**

Antar ALALIALKHALIL

**Thesis Advisor
Prof. Dr. Hayrettin AHLATCI**

**DETERMINATION OF FATIGUE STRESS OF ACCELERATED COOLED
S275 QUALITY PROFILE STEELS**

Antar ALALIALKHALIL

**Thesis Advisor
Prof. Dr. Hayrettin AHLATCI**

**T.C.
Karabuk University
Institute of Graduate Programs
Department of Metallurgical and Materials Engineering
Prepared as
Master Thesis**

**KARABÜK
Janurary 2024**

I certify that in my opinion the thesis submitted by Antar ALALIALKHALIL titled “DETERMINATION OF FATIGUE STRESS OF ACCELERATED COOLED S275 QUALITY PROFILE STEELS” is fully adequate in scope and in quality as a thesis for the degree of Master of Science

Prof. Dr. Hayrettin AHLATCI
Thesis Advisor, Department of Metallurgical and Materials Engineering

This thesis is accepted by the examining committee with a unanimous vote in the Department of Metallurgical and Materials Engineering as a Master of Science thesis.
January 31, 2024

<u>Examining Committee Members</u> (Institutions)	Signature
Chairman: Prof. Dr. Mustafa ACARER (SU)
Member : Assoc. Prof. Dr. Ismail Hakki KARA (KBU)
Member : Prof. Dr. Hayrettin AHLATCI (KBU)

The degree of Master of Science by the thesis submitted is approved by the Administrative Board of the Institute of Graduate Programs, Karabuk University.

Assoc. Prof. Dr. Zeynep ÖZCAN
Lisansüstü Eğitim Enstitüsü Müdürü

“I declare that all the information within this thesis has been gathered and presented in accordance with academic regulations and ethical principles and I have according to the requirements of these regulations and principles cited all those which do not originate in this work as well.”

Antar ALALIALKHAL

ABSTRACT

Master Thesis

DETERMINATION OF FATIGUE STRESS OF ACCELERATED COOLED S275 QUALITY PROFILE STEELS

Antar ALALIALKHALIL

Karabük University

Institute of Graduate Programs

Department of Metallurgical and Materials Engineering

Thesis Advisor:

Prof. Dr. Hayrettin AHLATCI

Janurary 2024, 52 pages

In this study, the changes in the microstructure and mechanical properties of S275JR quality steel profiles in sizes HEA 120 and HEB 120 to 140 after the "Accelerated Cooling and Self-Tempering (HS-KT)" heat treatment were examined. HS-KT heat treatment is carried out with a specially designed and manufactured system that sprays the air + water mixture onto the profile surface in a pulverized manner. HS-KT heat treatment was applied to the profiles at 12 bar air pressure 20 seconds cooling time. Microstructure examination of profiles with and without HS-KT applied was carried out by SEM analysis . Mechanical properties were determined by hardness measurement and flexure strength and fatigue tests. Hardness measurement was determined in HB with a 5 mm diameter ball under a load of 750 kg.

the Results show that the The fatigue strength decreases with increasing number of cycles for all three specimen geometries, following typical fatigue behavior. The fatigue limit increases slightly with thickness, from 564 MPa for the thinnest section to around 700 MPa for the thicker sections. Thickness increases the resistance of steel to both crack initiation and propagation mechanisms under cyclic stresses, leading to an improved inherent fatigue limit. An inverse relationship between hardness and thickness for the tested S275JR steel sections, with the thinnest HEB 120 displaying the highest hardness. Section size influences the mechanical properties. The HEA 120 section has the highest average flexural strength, followed by HEB 120 and HEB 140. The specific application and design requirements will dictate the significance of these results in practical use.

Key Word : S275JR alloy, Profile, structural steels , Accelerated Cooling and Self-Tempering, Microstructure, Mechanical properties.

Science Code : 91517

ÖZET

Yüksek Lisans Tezi

HIZLANDIRILMIŞ SOĞUTULMUŞ S275 KALİTE PROFİL ÇELİKLERİNİN YORULMA GERİLMELERİNİN TAYİNİ

Antar ALALIALKHALIL

Karabük Üniversitesi

Lisansüstü Eğitim Enstitüsü

Metalurji ve Malzeme Mühendisliği

Tez Danışmanı:

Prof. Dr. Hayrettin AHLATCI

Ocak 2024, 52 sayfa

Bu çalışmada HEA 120 ve HEB 120 ile 140 ebatlarındaki S275JR kalite çelik profillerin "Hızlandırılmış Soğutma ve Kendiliğinden Temperleme (HS-KT)" ısıtma işlemi sonrasında mikroyapısında ve mekanik özelliklerinde meydana gelen değişimler incelenmiştir. HS-KT ısıtma işlemi, hava + su karışımını profil yüzeyine toz halinde püskürten özel tasarım ve imalat sistemi ile gerçekleştirilir. Profillere 12 bar hava basıncında 20 saniye soğutma süresinde HS-KT ısıtma işlemi uygulandı. HS-KT uygulanmış ve HS-KT uygulanmamış profillerin mikroyapı incelemesi SEM analizi ile gerçekleştirildi. Mekanik özellikler sertlik ölçümü ve eğilme mukavemeti ve yorulma testleri ile belirlendi. Sertlik ölçümü HB'de 750 kg'lık bir yük altında 5 mm çapında bir bilya ile belirlendi.

Sonuçlar, tipik yorulma davranışını takiben, her üç numune geometrisi için döngü sayısı arttıkça yorulma mukavemetinin azaldığını göstermektedir. Yorulma sınırı

kalınlıkla birlikte hafifçe artar; en ince bölüm için 564 MPa'dan daha kalın bölümler için yaklaşık 700 MPa'ya kadar çıkar. Kalınlık, çeliğin döngüsel gerilimler altında hem çatlak başlatma hem de yayılma mekanizmalarına karşı direncini artırarak doğal yorulma sınırının iyileşmesine yol açar. Test edilen S275JR çelik bölümleri için sertlik ve kalınlık arasında ters bir ilişki vardır; en ince HEB 120 en yüksek sertliği gösterir. Kesit boyutu mekanik özellikleri etkiler. HEA 120 kesiti en yüksek ortalama eğilme dayanımına sahiptir, bunu HEB 120 ve HEB 140 takip etmektedir. Özel uygulama ve tasarım gereklilikleri, bu sonuçların pratik kullanımdaki önemini belirleyecektir.

Anahtar Sözcükler : S275JR alaşımı, Profil, yapı çelikleri, Hızlandırılmış Soğutma ve Kendiliğinden Temperleme, Mikroyapı, Mekanik özellikler.

Bilim Kodu : 91517

ACKNOWLEDGMENT

First of all, profusely all thanks be for ALLAH who enable me to achieve this work.

I would like to express my sincere gratitude to all those who have contributed to the completion of this thesis. First and foremost, I would like to thank my supervisor Prof. Dr. Hayrettin AHLATCI for his guidance, support, and encouragement throughout this research. I would also like to thank the participants who took part in this study and made this research possible.

Additionally, I would like to acknowledge the support of my family and friends who have been a constant source of motivation and encouragement.

Finally, I would like to express my appreciation to the institutions and organizations that provided funding and resources for this research.

This study has a great contribution to the installation of the accelerated watering system by TÜBİTAK 1005 project no. 222M441. At the same time, the examination of fatigue behavior of S275JR quality steels was supported by the project numbered KBÜBAP-23-YL-120 within the scope of Karabük University Scientific Research Projects Coordination Unit.

CONTENTS

	<u>Page</u>
APPROVAL.....	ii
ABSTRACT.....	iv
ÖZET.....	vi
ACKNOWLEDGMENT.....	viii
CONTENTS.....	ix
LIST OF FIGURES	xi
LIST OF TABLES	xii
SYMBOLS AND ABBREVIATIONS INDEX	xiii
PART 1	1
INTRODUCTION	1
PART 2	5
THEORETICAL BACKGROUND.....	5
2.1. IRON AND STEEL	5
2.2. IRON AND STEEL PRODUCTION IN THE WORLD AND IN TURKEY	6
2.3. IRON, STEEL PRODUCTION AND HISTORY	8
2.3.1. Integrated Plants – Basic Oxygen Furnace (BOF) Plants.....	9
2.3.2. Electric Arc Furnace	10
2.3.3. Facilities With Induction Furnace (IF).....	12
2.4. STRUCTURAL STEELS.....	12
2.5. QUENCHING AND SELF-TEMPERING APPLICATIONS.....	15
2.6. HEAT TRANSFER IN ACCELERATED COOLING OF STEEL PLATES.....	21
2.7. RESIDUAL VOLTAGE	22
PART 3	25
MATERIALS AND METHOD	25
3.1. MATERIALS	25

3.2. MATERIAL PREPARATION	26
3.3. APPLICATION OF HS-KT HEAT TREATMENT	27
3.4. MICROSTRUCTURE CHARACTERIZATION.....	30
3.5. HARDNESS MEASUREMENT	31
3.6. FATIGUE TEST	32
3.7. SHORT BEAM SHEAR METHOD	34
PART 4	37
RESULT AND DISSCSUION	37
4.1. INTRODUCTION.....	37
4.2. COOLING RATE	37
4.3. BRINELL HARDNESS	39
4.4. BENDING STRENGTH	40
4.5. FATIGUE TESTING	42
4.6. SEM IMAGES	44
PART 5	47
CONCLUSIONS	47
REFERENCES.....	48
RESUME	52

LIST OF FIGURES

	Page
Figure 2.1. Iron ores generally found in the earth's crust	5
Figure 2.2. Iron-carbon balance diagram.....	6
Figure 2.3. Development of steel production and forming technologies	9
Figure 2.4. Integrated iron and steel plant general production scheme	10
Figure 2.5. Electric arc furnace	11
Figure 2.6. Quenching and Self-Tempering (QST) for HISTAR steel grade principle of the process.....	17
Figure 2.7. Temperature change during the QST process	17
Figure 3.1. Cutting profiles to a length of 250 mm	26
Figure 3.2. Positions of holes drilled for thermocouples.....	27
Figure 3.3. Thermocouple mounted profile.....	28
Figure 3.4. Channel ADAM system	28
Figure 3.5. Heat treatment furnace.	29
Figure 3.6. SEM device.....	30
Figure 3.7. Brinell hardness device	31
Figure 3.8. Guided cantilever beam.	33
Figure 3.9. Short Beam Shear test setup.....	35
Figure 3.10. Typical damages encountered in the Short Beam Shear test.....	36
Figure 4.1. Cooling charts	38
Figure 4.2. Hardness change of the samples.	40
Figure 4.3. Bending strength of the samples	41
Figure 4.4. Fatigue strength of the samples.....	44
Figure 4.5. HEA120 quality 12 bar 20 sec. at 200 x SEM image magnification.....	45
Figure 4.6. HEB120 quality 12 bar 20 sec. at 200 x SEM image magnification.....	46
Figure 4.7. HEB140 quality 12 bar 20 sec. at 200 x SEM image magnification.	46

LIST OF TABLES

	<u>Page</u>
Table 2.1. Top 10 countries producing the most steel	7
Table 2.2. Chemical compositions of general structural steels	13
Table 2.3. Yield and tensile strengths of general structural steels.	14
Table 3.1. Profile characteristics	25
Table 3.2. Chemical composition of main material	26
Table 3.3. Heat treatment parameter	30
Table 4.1. Bending stree and maximum bending stress of the samples	42
Table 4.2. Cooling rates in the web, regions of the samples profile	43

SYMBOLS AND ABBREVIATIONS INDEX

SYMBOLS

h	: height
b.	: width
t	: wall thickness
Al	: Alminum
C _{EV}	: carbon equivalent
°C	: Degrees Celsius

ABBREVIATIONS

SEM	: Scanning Electron Microscope
ASTM	: American Society for Testing and Materials
HEA	: H Profile European Lightweight Wide Flange
HEB	: H Profile European Standard Wide Flange
CCT	: Continuous Cooling Transformation
QST	: Quenching and Self-Tempering

PART 1

INTRODUCTION

The accelerated cooling process has changed significantly in steel production in the last 30-35 years and has become an important process. This process was first used in the 1960s to shorten the rolling tables of hot rolled strips, but unexpected benefits were discovered. After the determination of these benefits, an intensive research study was started in this field and this process was examined from different perspectives.. Many types of steels, such as dual-phase steels, ferrite-bainite steels, and fine pearlitic steels, are products that have emerged as a result of the development of this process [1].

In our country, structural design codes were updated following a devastating earthquake in 1999. Reinforcing steel properties for concrete structures became an area of focus, and new specifications were introduced. One requirement limits the ratio of tensile strength to yield strength for S420 grade reinforcing bars to a maximum of 1.15. To satisfy this, the yield strength must exceed 420 MPa while maintaining tensile strength below this threshold ratio. A process called tempcore was developed to achieve the required properties profile. After rolling, steel bars pass through a water channel to rapidly cool outer surfaces. Within a subsequent cooling grid, heat from the core conducts quickly toward the shell, generating a uniform microstructure. This tempcore method enables reinforcing bars to meet the targeted yield strength threshold and simultaneously enhances toughness.

Careful control of phase transformations during accelerated cooling optimizes mechanical characteristics as defined in the revised structural design standards. Implementation of such processing technology helps reinforce earthquake resilience in infrastructure through upgraded material performance criteria [2].

Accelerated cooling process is used to increase the wear and fatigue resistance of pearlitic rails used within the scope of today's railway materials. The wear resistance of coarse pearlitic rails of eutectoid composition, known as R260 quality, is insufficient in bends with a radius of curvature below 2000 meters. In this context, a special cooling regime was determined and the material gained strength by narrowing the distances between perlite lamellae. In this way, the RS region on the rails, which had a hardness of 260-300 Brinell, reached 350-390 Brinell hardness, and the yield strength increased from 880 MPa to 1175 MPa [3, 4].

S355J2 quality HE type profiles are preferred as high-strength structural steels used in steel construction, road and railway vehicle manufacturing. These steels are also classified as general structural steels. These materials, which are used in a wide range of areas, from environments with high temperatures in summer to environments with harsh winter conditions, are needed in our country, especially at important points such as energy transmission lines. For S355J2 quality steels, a notch impact strength of 27 J is expected at -20°C. Since the billets produced by the closed casting method are not in contact with air during casting, they do not contain inclusions, unlike the open casting method. The billets, which are the raw materials of the 100x100x10 mm cross-section angle materials within the scope of this study, are produced by open casting methods [5].

S235JR, S275JR and S355JR quality building profiles in NPU, NPI, IPE, HEA and HEB geometry are among the frequently used building components in structural and many industrial areas such as construction, suspension bridges, tunnels and steel construction. In this study, it is aimed to combine high yield strength and good toughness properties for large material thicknesses with QST, one of the innovative production methods.

Within the scope of the study, the unheat-treated microstructures of HEA and HEB type S275JR quality steel profiles in different sizes have a ferrite + pearlite structure, and the strength values of these profiles are only suitable for low-loading industrial

use. However, for high-loading applications, profiles with higher wall thickness or high alloy profiles must be produced. In this case, both weight and cost increase. For this reason, within the scope of the study, "Accelerated Cooling Self Tempering (AC-ST)" process is applied to the profiles selected for the production of both light and strong profiles in the heat treatment stage, thus increasing both the strength values. as well as improvement in satiety is planned. For this reason, in order to design and manufacture the system that performs the heat treatment and to obtain optimum material mechanical properties, the distance between the cooling plate where the nozzles are placed and the profile was measured by water at city network pressure accompanied by 4, 8 and 12 bar air pressure and 10, 20 and 30 sec. Cooling times were determined as heat treatment parameters. It is anticipated that significant cost savings will be achieved in the industrial use of high-quality profiles produced with this method [5].

By carrying out the study, the necessary knowledge has been acquired regarding the strength increasing processes of steel profile manufacturers in Turkey. In addition, since the consumption of high-strength profiles in construction in Turkey is not sufficient and/or the use of these profiles is not made compulsory by regulations, necessary studies have not been carried out in the field of accelerated cooling and self-tempering. Making the use of both tough and strong steel more attractive in modern buildings and large projects in Turkey, as in the world, will be very beneficial for our country, which is in the earthquake zone.

H-beam is an economical cross-section and high-efficiency profile with more optimized cross-sectional area distribution and more reasonable strength-to-weight ratio. It got this name because its cross section is the same as the English letter "H". Because all parts of H-beam are arranged at right angles, H-beam has the advantages of strong bending resistance, simple structure, cost saving and light structure in all directions, and is widely used.

Its cross-section shape is similar to the economical cross-section profile of the capital Latin letter H, also known as universal steel beam, wide-sided (edge) I-beam or parallel flanged I-beam. The cross-section of H-beam generally consists of two parts: web plate and flange plate, also known as waist and edge [6].

The inner and outer sides of the H-beam flange are parallel or almost parallel, and the flange ends are at right angles, so it is called parallel flange I-beam. The thickness of the web of H-beam is smaller than that of common I-beam with the same web height, and the flange width is larger than that of common I-beam with the same web height, so it is also called wide-sided I-beam. Determined by its shape, section modulus, moment of inertia and corresponding strength of H-beam, it is clearly better than ordinary I-beam with the same single weight. When used in metal structures with different requirements, it shows superior performance whether exposed to bending moment, pressure load or eccentric load. Compared with ordinary I-beam, it can greatly increase the bearing capacity and save metal by 10% to 40% [6].

H-beams provide several benefits compared to other structural shapes. Their wide flanges can reduce material usage by 15-20% in lattice constructions. Parallel flange sides and perpendicular edge ends facilitate assembly and integration into components. This may decrease welding and riveting by approximately 25%, saving substantial time. Faster construction translates to shorter project timelines

Due to these advantages, H-beams are commonly employed, notably for:[6];

- i) Civil and industrial building structures such as large factories, warehouses, and modern high-rises requiring broader spans.
- ii) Industrial facilities where seismic resilience or high temperature working conditions are important.
- iii) Large bridge designs where high load-bearing capacity, sectional stability, and spans demand robust profiles.
- iv) Transportation infrastructure like highways and ship hulls. Additionally, foundation improvement, backfilling, and diverse machine parts.

PART 2

THEORETICAL BACKGROUND

2.1 IRON AND STEEL

The symbol of the iron element is Fe and its atomic number is 26. It is the fourth most abundant mineral in the world and the most abundant metal in the earth's crust. Iron is rarely found in metallic form in nature. The process of obtaining it in metallic form is provided by iron ores. Impurities in iron ores, which generally have an oxide structure, are removed from the structure by reduction. Today, in addition to being used on its own, iron is largely used in the production of steel, an alloy containing carbon.

Iron is found in the earth's crust at a rate of approximately 5%. Generally, iron ores found in the earth's crust are hematite, magnetite, goethite, limonite, pyrite and siderite Figure 2.1. [7].

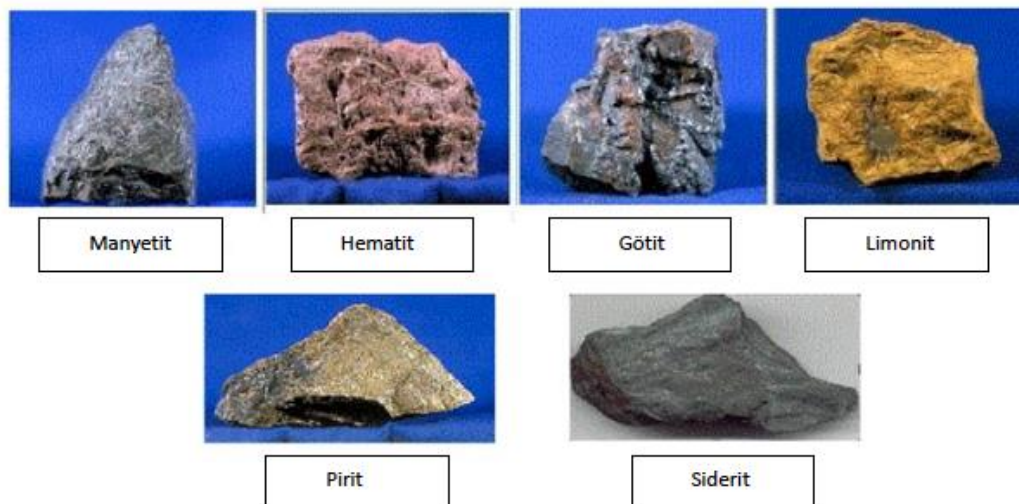


Figure 2.1. Iron ores generally found in the earth's crust [8].

Steel is essentially an iron carbon alloy. Carbon is present in iron at a rate of 0.02% to 2.06%, forming steel (Figure 2.2.). In addition to steel having many classification methods, the amount of carbon in the alloy plays an important role in this classification [9].

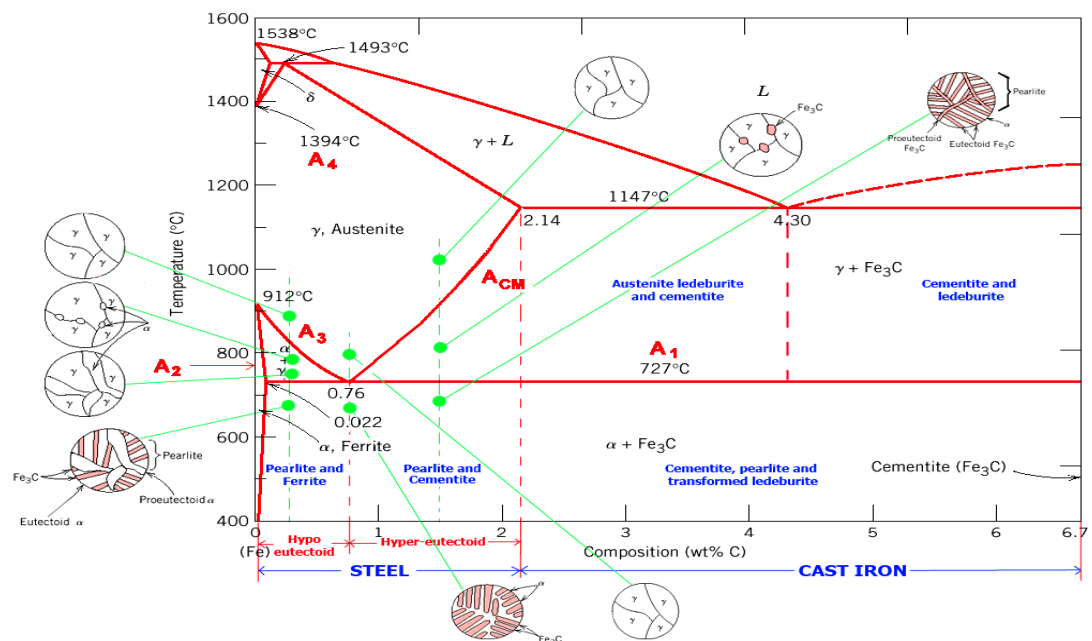


Figure 2.2. Iron-carbon balance diagram [10].

Although carbon is generally used as an alloying element in iron, different elements such as magnesium, manganese, silicon, chromium, vanadium, nickel, titanium and tungsten can also be used in alloying. With the addition of each element, values such as hardness, strength, toughness, yield and tensile strength of steel can be changed. Although these alloying elements are present in different amounts and in different forms in steel, they control properties such as ductility, hardness and stress point in steel. Today, steel and steel-based materials are among the most used materials in the world. It is widely used in buildings, automobiles, construction, infrastructure and superstructures, manufacturing sector, tools, ships, machines, accessories and weapons [8].

2.2 IRON AND STEEL PRODUCTION IN THE WORLD AND IN TURKEY

Turkey, which has an important place in the steel industry, has risen to 7th place in the world as of 2020 (Table 2.1.). Within the scope of the European Green Deal, which has become one of the subjects on which many studies have been carried out in the world recently, the iron and steel sector in our country, as well as other sectors within the metal industry, will be protected and developed until 2050, by protecting and improving competitiveness, creating new markets and producing more valuable products. Sectoral studies are continuing by the Ministry of Industry and Technology of the Republic of Turkey in order to become one of the countries with the highest technology in the world. In this context, especially recently, studies have been carried out to produce steel with low emission values [8].

Table 2.1. Top 10 countries producing the most steel

No	country	2019 Production (Mt)	2020 Production (Mt)	% Change (2020/2019)
1	Chinese	1001	1053	5
2	India	111	100	-11
3	Japan	99	83	-16
4	Russia	72	73	2.5
5	USA	88	73	-17
6	S.Korea	71	67	-6
7	Türkiye	33	36	6
8	Germany	40	36	-10
9	Brazil	33	31	-5
10	Iran	26	29	13

2.3 IRON, STEEL PRODUCTION AND HISTORY

The iron and steel industry is one of the world's most important and oldest production sectors in terms of tradition. Iron formed the basis of human culture and civilization about 3000 years ago. Today, the use of iron began before the period called the Iron Age. Iron production was first produced in Asia Minor, north of the Caucasus [11].

The advent of the water wheel in the 10th century revolutionized iron production technology. Hydraulic power has become more important than proximity to ore deposits. The first blast furnace experiments were seen in the 12th century, and commercial pig iron production here dates back to the early 14th century [12]. The important invention that has survived from past to present and contributed to the formation and development of civilizations and the change of social structures in human history is the production of steel by smelting iron [13].

18th century In Europe, where the industrial revolution took place until the 19th century, charcoal was used as a raw material in the production of iron and steel. For this reason, until this period, production facilities were established close to the forests around iron ore. In England, especially in the 18th century, coal, which has a higher heat energy potential than charcoal, was discovered as an alternative raw material that could be used in production due to the excessive felling of trees. With this development, production facilities began to be established close to coal deposits. In 1796, the first coke oven went into operation in Germany. Over time, innovations were made in production methods and technology. With the 'Bessemer production process' developed by British scientist Henry Bessemer in 1855, more durable and cheaper steel could be produced. In addition, the electric arc furnaces and integrated facilities that companies produce today were first put into operation during this period. Thus, by the end of the 19th century, revolutionary innovations occurred in the building industry (steel construction structures), transportation (sea, railway, road and air transportation) and defense industry (armored vehicles, submarines, etc.) [14]. As a result, serious breakthroughs in the iron and steel industry in Germany and England have shed light

on today's technological production. The development of steel production and forming technologies is shown in Figure 2.3 [15].

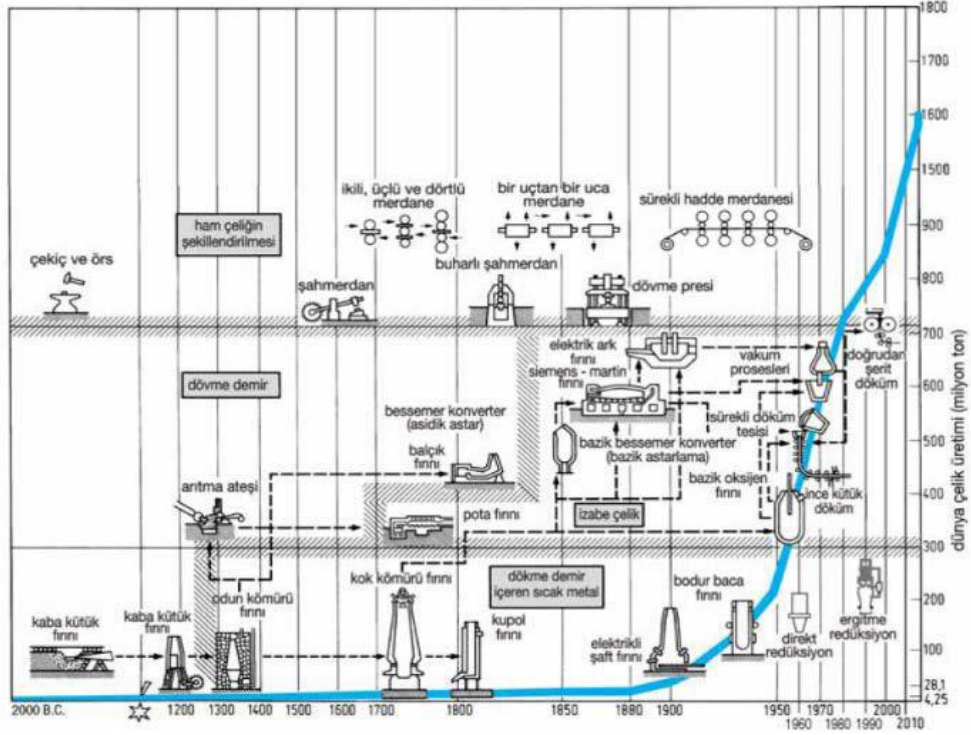


Figure 2.3. Development of steel production and forming technologies [5].

2.3.1 Integrated Plants – Basic Oxygen Furnace (BOF) Plants

The most common method for liquid steel production in the world is the basic oxygen furnace (BOF) method. In our country, this method is used in 3 large integrated iron and steel facilities: Erdemir, İsdemir and Kardemir. The basic raw material required for steel production is iron ore. In addition to iron ore, coking coal, one of the other required raw materials, is heated to a certain temperature in an oxygen-free environment in coke batteries to obtain metallurgical coke, and thus the resulting coke is ready for use in the blast furnace. Since ore cannot be fed in powder form in blast furnaces, there are sinter factories in facilities with blast furnaces that enable the

powder ore to agglomerate. However, after increasing the tenor content by enriching low-grade iron ores, turning the ores into pellets in pellet production facilities for use in blast furnaces is another agglomeration method. These raw materials are used together in blast furnaces and melted at certain temperatures, thus obtaining liquid iron. Pig (liquid) iron is passed through some processes in steel mill facilities where a basic oxygen furnace is located, and liquid steel is obtained, and billets and slabs are obtained from this liquid steel in continuous casting facilities. Slabs and billets are processed in rolling mills to obtain flat or long products and become final products. A general production pattern of integrated iron and steel plants is shown in Figure 2.4 [8].

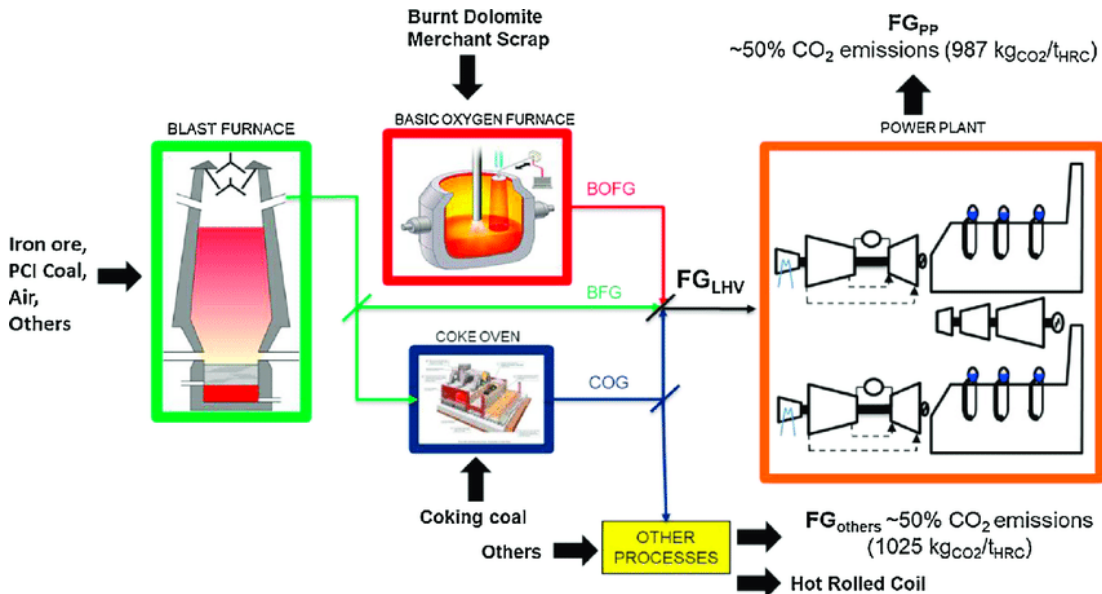


Figure 2.4. Integrated iron and steel plant general production scheme [8].

2.3.2 Electric Arc Furnace

In electric arc furnace facilities, liquid steel is produced using steel scrap. The scrap steel to be used in the furnace is unloaded into the furnace from the upper area with the help of a crane, and then the furnace cover is closed. This cover carries the electrodes immersed in the arc furnace. The electric current passing through the

electrodes creates an arc and the resulting heat melts the scrap. The molten metal is then subjected to crucible metallurgy to add alloying elements. The liquid steel prepared in ladle metallurgy is then transferred to continuous casting facilities to obtain intermediate products such as billets or slabs. The general scheme of electric arc furnace facilities is given in Figure 2.5 [8].

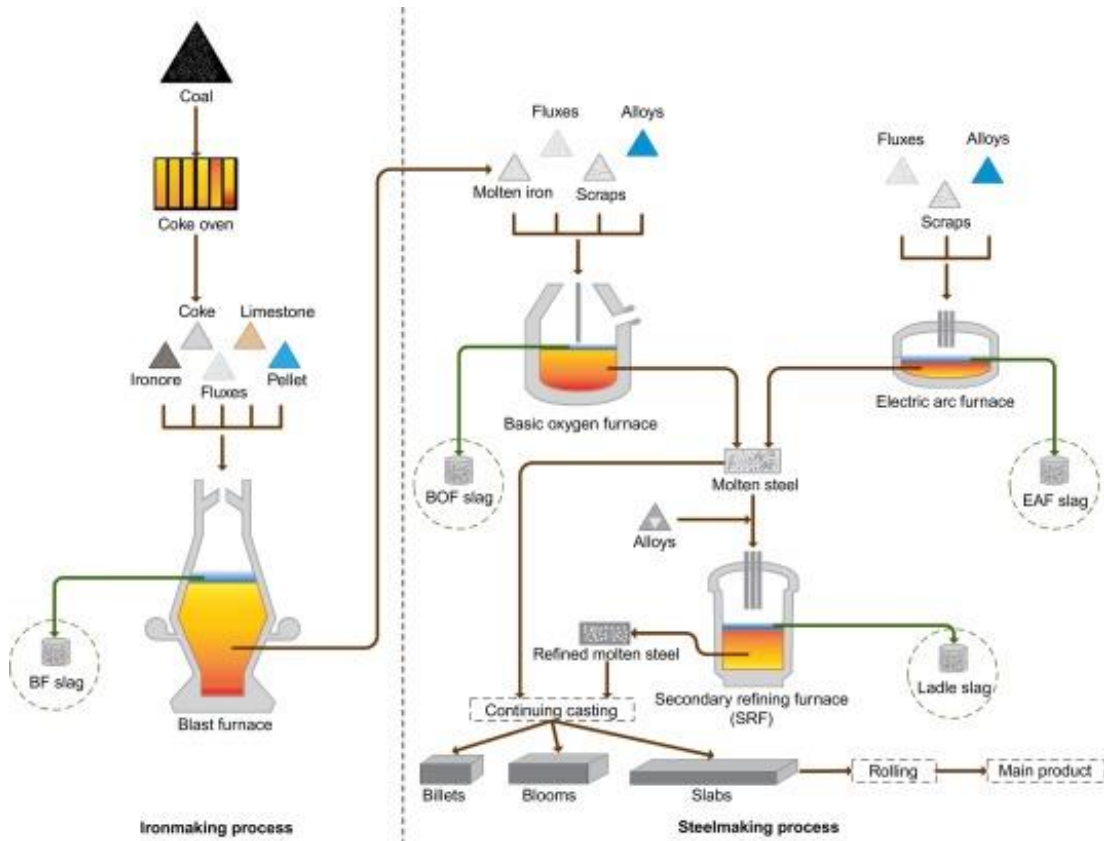


Figure 2.5. Electric arc furnace [16].

2.3.3. Facilities With Induction Furnace (IF)

In induction furnace production processes, steel production is carried out by melting steel scrap. Scrap steel is unloaded into the upper area of the melting furnace using a crane, then the furnace door is closed. After the molten metal is taken from the arc furnace, the crucible metallurgy process is carried out to add alloying elements. The liquid steel obtained in the ladle metallurgy process is transferred to continuous casting facilities and billets or slabs are produced here [8].

2.4 STRUCTURAL STEELS

The beginning of the use of steel in multi-storey building construction dates back to the late 1800s. The steel structures built in Chicago in 1888 are the 14-storey Tacoma Building and then the 39.32 meter high Tower Building in New York. The reason for the gradual increase in the number of floors of business centers called skyscrapers in these years and until the late 1920s was the discovery of the advantages of soft carbon steel used in steel structure design in terms of strength and ductility compared to materials such as cast steel and forged steel. Thanks to technological developments in rolling methods, the production of large profiles and the construction of high-rise steel structures have become more economical [17].

Structural steels account for the largest proportion of steel production in the world. In these steels, which are referred to as unalloyed, elements such as nitrogen and phosphorus, as well as manganese, silicon, sulfur and copper elements resulting from production, are also very effective [18]. Chemical compositions of structural steels according to TS EN 10025-2 standard are given in Table 2.2.

Table 2. 2. Chemical compositions of general structural steels [5].

Designation		Method of deoxidation	C in % max. for nominal product thickness in mm			Si % max	Mn % max	P % max	S % max	N % max	Cu % max	other % max (g1)
Steel name	Steel number		≤ 16	> 16 ≤ 40	> 40 C							
S235JR	1.0038	FN	0,19	0,19	0,23	-	1,50	0,045	0,045	0,014	0,60	
S235J0	1.0114	FN	0,19	0,19	0,19		1,50	0,040	0,040	0,014	0,60	
S235J2	1.0117	FF	0,19	0,19	0,19		1,50	0,035	0,035		0,60	
S275JR	1.0044	FN	0,24	0,24	0,25	-	1,60	0,045	0,045	0,014	0,60	
S275J0	1.0143	FN	0,21	0,21	0,21 h		1,60	0,040	0,040	0,014	0,60	
S275J2	1.0145	FF	0,21	0,21	0,21 h	-	1,60	0,035	0,035		0,60	
S355JR	1.0045	FN	0,27	0,27	0,27	0,60	1,70	0,045	0,045	0,014	0,60	
S355J0	1.0553	FN	0,23	0,23 i	0,24	0,60	1,70	0,040	0,040	0,014	0,60	
S355J2	1.0577	FF	0,23	0,23 i	0,24	0,60	1,70	0,035	0,035		0,60	
S355K2	1.0596	FF	0,23	0,23 l	0,24	0,60	1,70	0,035	0,035		0,60	
S460JR	1.0507	FF	0,23	0,23 l	0,24	0,60	1,80	0,040	0,040	0,027	0,60	k
S460J0 j	1.0538	FF										
S460J2 l	1.0552	FF										
S460K2 j	1.0581											
S500J01	1.0502	FF	0,23	0,23	0,24	0,60	1,80	0,040	0,040	0,027	0,60	k

Structural steel classes are shown with the symbol SXXX in the EN 10025 standard. Structural steels, expressed according to yield strength, are primarily taken into account by their tensile strength and yield limit values and have a wide range of usage in welded steel structure manufacturing. The number (XXX) in the steel type expression refers to the minimum yield strength of the steel in N/mm^2 unit in the tensile test performed on elements whose thickness does not exceed 40 mm. For example, for S235 quality, the minimum yield strength of steel is $235 N/mm^2$, that is, $2350 kgf/cm^2$. Although there are many steel grades, the most commonly used structural steel type is S235 quality. When choosing general structural steel at the design stage, the steel semi-finished product dimensions to be used in Tables 2.3 and 2.4 should be taken into consideration [18].

Table 2.3. Yield and tensile strengths of general structural steels [5].

Designation		Minimum yield strength MPa Nominal thickness										Tensile strength MPa Nominal thickness				
Steel name	Steel number	s 16	> 16 40	> 40 s 63	> 63 s 80	> 80 s 100	> 100 150	> 150 s 200	> 200 s 250	> 250 s 400	< 3	> 3 s 100	> 100 s 150	> 150 s 250	> 250 s 400	
S235JR	1.0038															
S235JO	1.0114	235	225	215	215	215	195	185	175	165	360 to 510	360 to 510	350 to 500	340 to 490	330 to 480	
S235J2	1.0117															
S275JR	1.0044															
S275JO	1.0143	275	265	255	245	235	225	215	205	195	430 to 580	410 to 560	400 to 540	380 to 540	380 to 540	
S275J2	1.0145															
S355JR	1.0045															
S355JO	1.0553															
S355J2	1.0577	355	345	335	325	315	295	285	275	265	510 to 680	470 to 630	450 to 600	450 to 600	450 to 600	
S355K2	1.0596															
S460JR b	1.0507															
S460JO b	1.0538															
S460J2 b	1.0552	460	440	420	400	390	390	-	-	-	-	550 to 720	530 to 700	-	-	
S460K2 b	1.0581															
S500JO b	1.0502	500	480	460	450	450	450	-	-	-	-	580 to 760	560 to 750	-	-	

Table 2. 4. Toughness values of general structural steels [5].

Designation		Temperature	Minimum energy Nominal thickness in mm		
Steel name	Steel number		≤ 150 ab	> 150 ≤ 250b	> 250 ≤ 400
S235JR	1.0038	20	27	27	27
S235J0	1.0114	0	27	27	27
S235J2	1.0117	-20	27	27	27
S275JR	1.0044	20	27	27	27
S275J0	1.0143	0	27	27	27
S275J2	1.0145	-20	27	27	27
S355JR	1.0045	20	27	27	27
S355J0	1.0553	0	27	27	27
S355J2	1.0577	-20	27	27	27
S355K2	1.0596	-20	40	33	33
S460JR^e	1.0507	20	27		
S460J0^e	1.0538	0	27		
S460J2^e	1.0552	-20	27		
S460K2^e	1.0581	-20	40		
S500J0^e	1.0502	0	27		

2.5. QUENCHING AND SELF-TEMPERING APPLICATIONS

The QST (Quenching and self-tempering) unit in the heavy profile mill of ArcelorMittal, one of the world's leading steel producers, has been in operation for 30 years. Thanks to this unit, the combination of high strength, ductility and excellent weldability properties in steel production, improvement in design parameters and buckling curves by using thick heavy profiles called jumbo in wide-span space frame

elements and heavy load-bearing building columns, contribution to fire engineering, high-strength steel quality H Combining profiles with high-strength concrete has increased the life of high-performance composites and bridges [19].

Under the name of "Quenching and Self-Tempering" process, the cooling processes exhibited abroad by a limited number of companies such as ARBED (LUXENBURG), CRM (BELGIUM) and BRITISH STEEL (GREAT BRITAIN) are carried out with the formation of a dense water pillow and have been successful to date. results are obtained. It is also marketed under the brand HISTAR® (High STrength ARcelor) and is defined as high-strength steel among the conventional structural steels included in the national standards of Europe and America with the codes EN10113-3:1993, ASTM A913-01 and DIN 18800-7:2002, and its performances are Steel profiles produced in this fully accepted steel quality have been used extensively in Europe since the first day in special applications such as steel elements of wide-span space roofs, heavy-load-bearing "Jumbo" section steel columns of high-rise buildings, deep steel beams of composite bridges, steel ground piles of deep foundations. It has been used with success [19-21].

With the quenching and self-tempering (QST) system given in Figure 2.6, intense water cooling is applied to the entire surface of the beam after the last pass of the tandem mill, where the profiles are taken to their final dimensions [22].

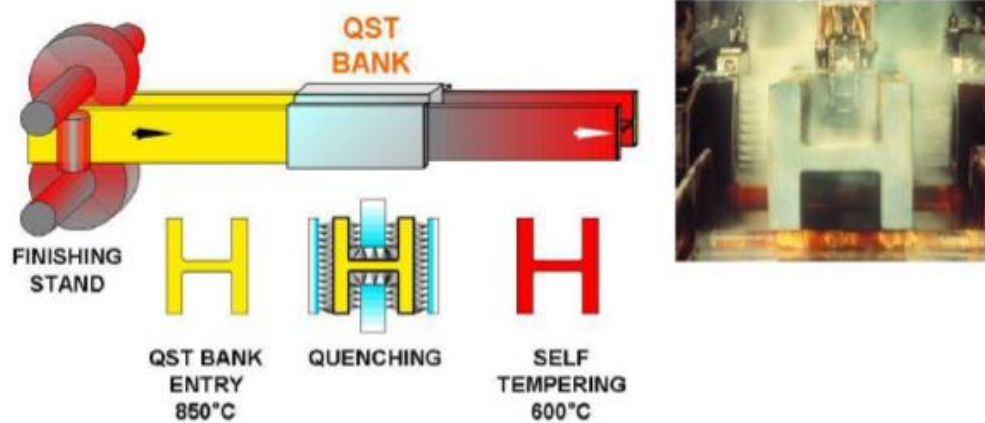


Figure 2.6. Quenching and Self-Tempering (QST) for HISTAR steel grade principle of the process [22, 23].

In Figure 2.7, before the core is affected, cooling is interrupted and the outer layers are annealed by heat flow from the core to the surface. At the exit of the tandem mill, directly at the inlet of the QST unit, the temperature of the material is typically 850°C. After quenching the entire surface of the profile, it is self-tempered at 600°C [24].

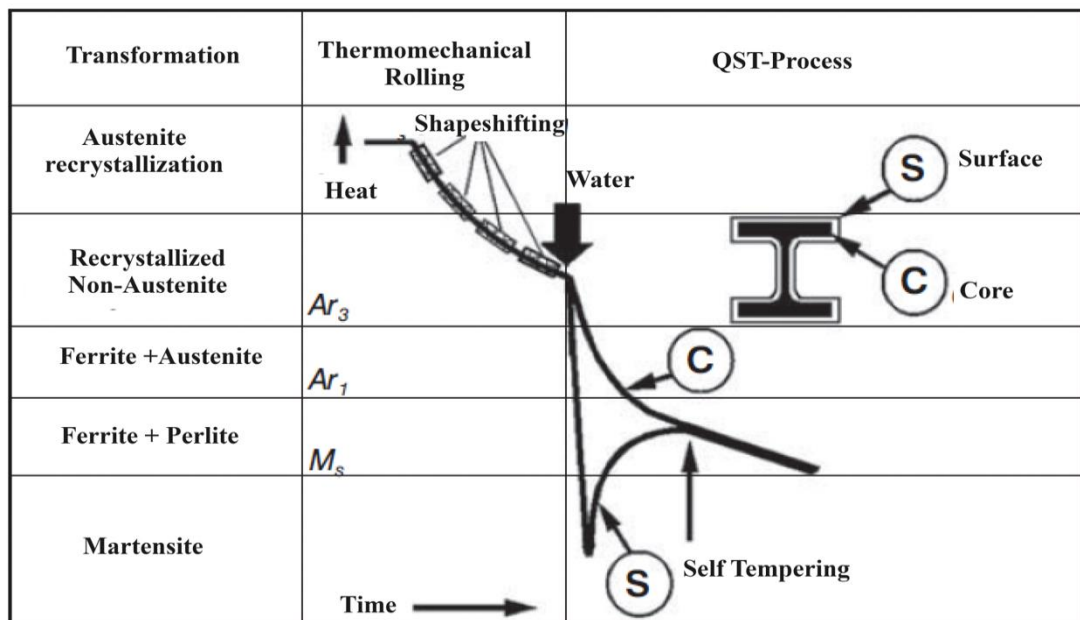


Figure 2.7. Temperature change during the QST process [24].

HEA and HEB profiles made with S275JR steel grade are commonly used in the construction of buildings, bridges and tunnels due to their strength and structural properties [24]. While previous studies have investigated water for cooling applications, no research was found on using a water-air mixture for quenching as performed in this study [25]. Producing high-strength structural steels requires advanced manufacturing techniques and stringent quality controls to ensure safety-critical applications [26, 27].

Thermomechanical processing enables developing material properties like high strength and toughness simultaneously, which were previously considered incompatible. Through careful control of thermal cycles, yield strength can be increased without losing toughness or weldability. Building on this, a manufacturer patented a proprietary process to produce heavy sections with these combined attributes [28, 29].

The process involves controlled cooling to temper the surface layers while allowing equilibration between the core and outer skin. This technique can fabricate heavy-walled wide flange profiles from high-strength grades that may otherwise be difficult to process. Continuous advances in thermal treatment methods now facilitate manufacturing structural steel at higher specifications than previously achievable to meet the growing demands of modern infrastructure projects. Precisely how innovative processes like this promote microstructural development warrants further exploration [5].

After heat treatment during the austenitization and quenching process, it is expected that the steels will have a microstructure such as bainite, containing a fine dispersion of ferrite and pearlite due to the rapid cooling rate. This microstructure typically combines high strength with high toughness [30]. Currently, high-pressure water spraying is commonly used in quenching and tempering units. However, limited information is available on operating parameters for alternative cooling methods. No prior studies were found examining the use of a water-air mixture for cooling.

Therefore, this study aims to evaluate such a mixed-fluid system, which could provide energy savings over water-only quenching while achieving comparable metallurgical outcomes:

Snijder et al [31] examined properties of quenched and tempered heavy steel sections. One study evaluated existing buckling design recommendations for stocky steel columns fabricated from mild and higher strength grades. As current design codes lack guidance for slenderness ratios above 1.2 or flange thicknesses over 100mm, finite element models were used to develop new buckling curves, accounting for residual stresses developed during manufacturing. This involved simulating the mechanical behavior of a wide range of column geometries to establish appropriate resistance factors.

Various wide flange profile types were investigated with flange thicknesses exceeding 100 mm, including thinner HL sections ($h/b = 2.35$) and heavier HD sections ($h/b = 1.23$). Materials studied included quenched and tempered steels under various proprietary grades developed for enhanced properties, such as HISTAR 460 (High Strength ArcelorMittal) with a yield strength of 460 MPa. Additional grades evaluated were QST S460, S355 and S235 steel.

Where available, statistical data on material properties were referenced to estimate the partial factor (γ_m) for each grade. The analysis factor (γ_{M1}) was then calculated as the product of γ_m and the resistance factor (γ_{Rd}) derived previously. Eurocode design recommendations specify γ_{M1} should not exceed 1.05. Accordingly, proposed buckling curves were developed targeting a γ_{M1} of 1.0 for use in EN 1993-1-1 specifically for stocky columns beyond the current scope of height-to-width ratios over 1.2 and flange thicknesses above 100 mm [31].

Seung Hoon et al. [32] investigated the impact of non-uniform water cooling on the dimensional stability of rolled H-beam sections. The Quenching and Self-Tempered (QST) process is an advanced thermomechanical treatment that enhances the strength and toughness of structural shapes. However, in some cases rapid cooling during QST

can create irregularly distorted cross-sections, sometimes called "wacky square" deformations, due to uneven temperature differentials developing across the profile.

it observed a correlation between non-uniform cooling rates during QST processing and shape deformation. Finite element modeling software was used to computationally simulate deformation mechanisms in profiles by combining thermal expansion effects and volume changes associated with phase transformations during accelerated cooling. Direct measurements were also made and compared to simulation results to validate the model's predictive capability. The findings provided insight into how rapid increases in temperature gradients and localized stresses influenced distortion behaviors in H-beams. Optimizing cooling uniformity during thermomechanical processing stands to minimize undesirable shaping deviations and maintain dimensional accuracy of rolled structural sections for fabrication.[32].

In another study, the bending behavior of hot-rolled H-beams after quenching and self-tempering was investigated. Rather than deformations induced during hot rolling, the focus was on warping that could result from thermometallurgical and mechanical effects of rapid cooling. Finite element modeling was used to simulate quenching of several representative H-beam cross-sectional profiles commonly encountered in manufacturing.

To analyze the impact of accelerated heat treatment and associated phase transformations on bending, transient quenching simulations were performed using modeling software. Theoretical considerations like latent heat release during quenching, heat transfer dynamics, and phase changes accompanying temperature variations were incorporated. The computational predictions were then compared to experimental measurements to validate the simulation's effectiveness in elucidating the underlying bending mechanisms.[33] Further analyses using the simulation were conducted to better understand what factors might induce unexpected distortions. Accounting for metallurgical phenomena like material phase transitions in addition to thermal gradients and stresses holds potential for optimizing quenching parameters to minimize undesirable deformations in structural sections during heat treatment operations [33].

In literature study, Harman [34] the suitability of different welding techniques for joining QSTE 420TM high-strength steel sheet was investigated. Maintaining the exceptional strength properties of this fine-grained alloy steel after fabrication is important. Several factors influence weldability, including base material composition/thickness, welding process selected, filler metal chemistry/properties, and heat input level. By optimizing these parameters, welding procedures were developed and butt joints tested under 3 groups employing metal active gas, tungsten inert gas, and gas metal arc welding respectively. Following metallographic examination and mechanical testing of test joints, the most effective technique in each category was identified based on the strength attained relative to the base material. The welding methods and conditions suitable for manufacturing structures from QSTE 420TM sheets while preserving the inherent strength advantages this steel offers. Careful control of variables made certain processes more compatible than others for specific applications depending on design requirements. This provides guidance on joining strategies that minimize weakening effects in high-performance fabricated structures.[34].

2.6 HEAT TRANSFER IN ACCELERATED COOLING OF STEEL PLATES

Using modern cooling systems, it has become very easy to achieve cooling rates higher than almost 100 °C per second. While these cooling processes are carried out much more easily in plates with thin sections, as the section thickness increases, heat transfer will become more difficult and the cooling process will take time. The two main components that affect this process are the residual stresses occurring throughout the thickness of the plate and the microstructural properties. In thin-section plates, the critical factor is the heat transfer on the surface. Above 450 °C, a stable vapor layer with a high cooling rate forms on the surface of the plates. At temperatures below 450 °C, the vapor layer will break and the heat transfer rate will increase. Below 150 °C, boiling disappears and the heat transfer rate decreases again. A gradual cooling process is applied between 800-500 °C. Direct quenching is carried out at temperatures between 200-900 °C. As a result, it is necessary to reach a sufficient speed in cooling

the plates in order to obtain the martensitic structure. When the specified conditions are met, the cooling rate will become easily controllable.

20% of steel plates are produced by rolling with this method. Nowadays, accelerated cooling is widely used for the production of steel plates with a thickness of only up to 100 mm. With this method, high-strength steel plates with a tensile strength of more than 490 MPa can be obtained. That's why these plates are used in shipbuilding, offshore platforms, API pipes, high-rise buildings, bridges, pressure pipes, low temperature tanks, cryogenic tanks and heavy duty machines. These products and technical data standards are accepted in many steel production factories in global sectors. After almost 30 years, cooling and quenching processes have accelerated after industrial applications were disrupted. New formations of the mechanical properties and alloy contents of the materials enable the optimization of such processes and it is possible to produce high-quality steel plates.

2.7 RESIDUAL VOLTAGE

Residual stresses are elastic stresses that remain in the part after various production/manufacturing stages. Plastic deformations or thermal changes that are not distributed homogeneously in the material as a result of welded manufacturing, casting, surface treatments and heat treatments are the main reasons for the formation of residual stress [35].

In a 3D material, deformation occurs in all three different dimensions. If the change in the resistance of the material is examined with this method, unfortunately it will be impossible to understand what size of deformation is in which axis. In addition, the larger the part dimensions, the more impossible direct measurement will be. For this reason, an auxiliary element is needed to make measurements on a desired axis. The name of this auxiliary element is the Residual Tension Meter Rosette (Strain-Gage Rosette). This material is insulated elements containing a wire of circular cross-section oriented in one direction. We can stick this badge on the part we want to measure in

any direction we want, measure the resistance change, and in this way calculate the unit strain [36].

Residual stresses are stresses locked within a metal object even though the object is free from external forces. Residual stresses are formed as a result of the confinement of a region of metals from expansion, contraction or release of elastic stresses by adjacent regions. Residual stresses may occur in tension or compression. Tensile and compressive residual stresses coexist within a component. Residual stresses occur when a component is stretched beyond its elastic limit and plastic deformation occurs. Plastic deformation occurs when stress exceeds the yield strength limit of a metal.

In parts cooled rapidly from high temperatures, residual stresses occur due to sudden temperature changes in the steel during cooling. Cooling from high temperatures generally occurs during heat treatment and welding applications. 13 Temperature changes when a metal is cooled from high temperatures cause the amount of thermal contraction to change locally. Thermal shrinkage is equal to non-uniform stress due to different cooling rates occurring on the surfaces and interior surfaces of metals such as steel rectangular profiles. During cooling, the outer part of a component cools first and this area of the metal contracts and the hot inner surface compresses the metal, creating stress. As the interior of the component cools, the metal attempts to contract, but with the pre-cooled exterior, shrinkage remains limited. As a result, the outer part will have a residual compressive stress, while the inner parts will have a residual tension.

Phase transformation refers to alterations in the metallic phases making up an alloy. For example, the conversion of austenite to martensite during steel hardening represents a phase change. Residual stresses arise from volumetric mismatches between newly forming and original metallurgical phases during transformation.

The disparity in molar volumes gives rise to expansion or contraction of the material. Rapid cooling processes like quenching initiate phase changes beginning at external

surfaces before progressing inward. When the volume of the product phase differs from the initial phase, conversion induces dimensional changes.

As internal regions cool, they attempt to alter size but are constrained by already-transformed exterior layers. A larger product phase volume compresses the core under exterior traction. A smaller volume places the core in tension against compressive exterior layers. For instance, steel quenching converts austenite (4% smaller volume) to martensite initially on surfaces as they rapidly cool. Subsequent transformation internally expands against immobilized surface layers, inducing tensile core stresses and compressive surface stresses.

In some cases, transformation-induced volume changes can generate plastic deformation and warping if stresses exceed yield strength. Severe quenching may even cause cracking. Control of processing seeks to optimize microstructural development while mitigating distortion and failure from thermal stresses. Residual stresses also arise due to non-uniform plastic deformation across a component's cross-section during forming processes like bending, tension/compression, rolling, and extrusion. When a material experiences plastic deformation, a portion of the strain is elastic (as discussed in tensile testing studies).

After unloading, the material attempts to recover this stored elastic energy. However, complete recovery is impeded by neighboring sections that underwent permanent plastic deformation. Consider a pre-bent metal object. Regions beside the curved segment only deflect elastically and regain their shape upon load removal through a phenomenon known as springback. However, permanent bending of adjacent material inhibits full shape recovery of the elastic regions back to an undeformed state. These elastic regions become trapped in tension, with plastically deformed areas now in compression. Redistribution of stresses during plastic straining followed by constrained elastic unloading leaves residual stresses induced within nonuniformly deformed components. [6].

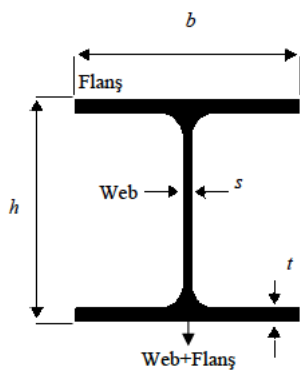
PART 3

METHODOLOGY AND EXPERIMENT

3.1 MATERIALS

In this study, steel structure profiles of S275JR quality HEA 120 and HEB 120 to 140 sizes, which are the most commonly used in steel construction structures, were used. S275JR quality beam blanks with dimensions of 280X360X90 mm used in the production of profiles were cast in continuous casting facilities as open casting and without vacuum. These semi-finished products were shipped to the rolling mill and subjected to annealing at 1200°C. They were produced by passing in reversible rolling mills using the hot rolling method after the annealing process. The dimensions of the HEA 120 and HEB 120/140 profiles produced are given in Table 3.1.

Table 3.1. Profile characteristics



	h	b	s	t	Unit Mass (kg/m)
114	120	5	8	19.9	
120	120	6.5	11	26.7	
140	150	7	12	33.7	

The chemical composition (% by weight) of the profiles used is given in Table 3.2. The profiles were produced according to the EN 10025-2 standard and their chemical compositions were found to comply with the standard

Table 3.2. Chemical composition of main material

Materials	C	Mn	Si	S	P	Cr	Ni	Cu	V	Al	Nb	C _{ev}	N
HEA120	0.094	0.75	0.12	0.01	0.01	0.04	0.04	0.06	0.002	0.001	0.0002	0.23	68
HEB140	0.10	0.71	0.07	0.02	0.01	0.03	0.04	0.04	0.0009	0.001	0.0002	0.23	58
HEB140	0.09	0.91	0.17	0.02	0.01	0.03	0.03	0.03	0.005	0.001	0.0003	0.25	60

3.2. MATERIAL PREPARATION

The HEA 120/140 and HEB 120/140 sized S275JR quality steel structure profiles to be used in the thesis study were cut with a KARMETAL brand 220 KDG model band saw (Figure 3.1) in 250 mm length to be suitable for transportation during the HS-KT heat treatment to be applied.



Figure 3.1. Cutting profiles to a length of 250 mm.

In order to monitor the temperature change during the HS-KT heat treatment of HEA 120 and HEB 120/140 size S275JR quality steel profiles, holes suitable for the diameter of the insulator attached to the end of the thermoculps were opened with a drill in the web, web+flange and flange regions given in Figure 3.2.



Figure 3.2. Positions of holes drilled for thermocouples.

3.3 APPLICATION OF HS-KT HEAT TREATMENT

After the HS-KT heat treatment system was installed, thermocouples were attached to the holes drilled in HEA 120/140 and HEB 120/140 sized S275JR quality steel profiles to control temperature distributions during the accelerated cooling process. Figure 3.3 shows the profile on which the thermocouples are attached.



Figure 3.3. Thermocouple mounted profile.

In temperature measurements, K-type thermocouple wires, which can measure 1500°C, were attached to the specified points with polymer-based adhesives and the temperature was recorded for each second with the help of the 16-channel ADAM system and software given in Figure 3.4.



Figure 3.4. Channel ADAM system.

For the HS-KT heat treatment, the profiles cut to 250 mm in length, with holes drilled and thermocouples attached, were first austenitized in a muffle furnace with a volume of 290x290x450 mm³ with a Telmika model temperature control unit in Figure 3.5, where the temperature distribution is minimum. It is important that the temperature distribution in the austenitizing furnace is minimum in order to obtain optimum mechanical properties along the cross-section of the profiles to be austenitized and HS-KT heat treated. In addition, the austenitizing process in the furnace atmosphere was carried out under the atmosphere of N₂-5H₂ gas mixture . 950°C was selected as the austenitizing temperature of the examined profiles, and the austenitizing time was determined according to the general 1-hour annealing heat treatment rule for 1 inch thickness .



Figure 3.5. Heat treatment furnace .

Within the scope of the thesis study, 3 different test parameter groups: Cooling Time, Distance Between Cooling Plate and Profile and Air Pressure were applied to HEA 120 and HEB 120/140 sized S275JR quality steel profiles. Heat treatment parameters are given in Table 3.3. In the study, 20 sec. was used HS-KT heat treatment was applied at different cooling times, 2 layers of cooling plate profile distance, 12 bar air pressure.

Table 3.3. Heat treatment parameter .

Profile	Temperature (°C)	Cooling Time (sec.)	Distance Between Cooling Plate and Profile (mm)	Air Pressure (Bar)
HEB 120	950	20	2 Kat 120 mm	
HEB 140			2 Kat 140 mm	12
HEA 120			2 Kat 120 mm	

3.4 MICROSTRUCTURE CHARACTERIZATION

For metallographic processes, samples of 25x15x10 mm dimensions were cut from heat-treated profiles. The prepared samples were prepared for polishing by sanding in the 400-2500 mesh range and were polished with 3 micron Al₂O₃. Microstructure examination (SEM - Optical): Here, the samples to be cut to certain sizes will be examined with the Carl Zeiss Ultra Plus Gemini Fesem model ZEISS brand SEM imaging device located at Karabük University MARGEM Institute, and the microstructures of the casting as well as artificially aged and thermomechanically artificially aged materials will be examined.



Figure 3.6. SEM device.

3.5 HARDNESS MEASUREMENT

The cross-sectional surfaces of the profile pieces resulting from the residual stress measurement were used for hardness measurement. Hardness values were measured for 10 seconds in accordance with the standard on the OPTOBUL brand device in Figure 3.7. It was measured in Brinell with a 5 mm ball under a load of 750 g for a period of time.



Figure 3.7. Brinell hardness device.

Hardness tests were carried out on the web region of the section of the original (non-heat treated) profiles that were subjected to accelerated cooling, as shown in Figure 3.7. The average values of hardness measurements taken from at least 3 different points in each region in the web region was taken.

3.6 FATIAGUE TEST

We conducted a fatigue test using a custom-built testing rig in our lab. The rig consists of two opposing grips - one fixed and one movable. A motor is used to drive the movable grip in a cyclic movement. Data acquisition software on the rig allows the user to control and record the cycling frequency. Our rig applies a repeating bending load of constant amplitude to the specimen by moving the grips cyclically. The maximum and minimum displacement limits are set manually using adjustable bolts on the grips.

The rig loads the sample in a cyclic fashion and simultaneously counts the number of load cycles. When the sample fractures, the number of cycles completed is noted. This data is then used to create an S-N or Wöhler curve for the material. Commonly known as an S-N curve, this is a graph with stress amplitude on the x-axis and number of cycles to failure on the y-axis, both generally displayed on a logarithmic scale.

For each test material, we plotted a curve showing the relationship between the cyclic stress level and the number of stress cycles sustained prior to fracture. This provided insight into the fatigue performance and life of the material under different loading conditions.

stress amplitude is calculated by the equation:

$$\sigma = E \frac{6\sigma h}{L^2}$$

This law was arrived at from the following relations

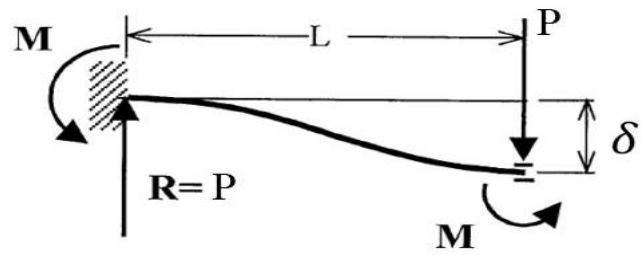


Figure 3.8. Guided cantilever beam [26].

$$\text{Equivalent bending stress } \sigma = \frac{M_b}{I} y$$

$$M_b = PL \quad , \quad I = \frac{bh^3}{12} \quad , \quad y = \frac{h}{2}$$

$$\rightarrow \sigma = \frac{PL \frac{h}{2}}{\frac{bh^3}{12}} \rightarrow \sigma = 6 \frac{PL}{bh^3}$$

$$P = 12 \frac{EI}{L^3} \delta \rightarrow \sigma = 6 \frac{12 \frac{EI}{L^3} \delta L}{bh^3} = \frac{12 \frac{E}{L^3} \frac{bh^3}{12} \delta L}{bh^3} = 6 \frac{E\sigma h}{L^2}$$

$$\sigma = E \frac{6\sigma h}{L^2}$$

E : Young's modulus [N/m²]

δ : max. amount of bending deformation [m]

b : width of the sample [m]

h : Thickness of the sample [m]

L : Distance between supports [m]

3.7 SHORT BEAM SHEAR METHOD

Short Beam Shear Method is also called Three Point Bending. This method is used to determine the interlayer shear strength of fiber-reinforced polymer matrix layered composite materials. The method used in the thesis was approved by the ASTM D 30 committee in 2006. Interlaminar shear strength iS is calculated as defined in the Short Beam Shear test method ASTM D 2344.

The test setup for the ASTM D 2344 standard is seen in Figure 3.9. The diameter of the supports should be 3 mm and the diameter of the cylinder loading head should be 6 mm. The supports and the loading cylinder head must be overhanging the sample by at least 2 mm on both sides. The parts of the sample outside the support must be at least as thick. Loading continues until either the sample is damaged and breaks into two pieces, or until the load value drops by more than 30%.

In the ASTM D 2344 standard, an s/t ratio is defined by calling the distance between the supports s and the thickness of the sample as t . When the s/t ratio is between 4 and 8, Short Beam Shear test can be applied. The standard recommended ratio is 4 or 5. If the s/t ratio is less than 4, compression damage occurs, and if it is greater than 8, flexibility damage occurs. Recommended sample sizes;

Sample length = thickness x 6

Sample width = thickness x 2.

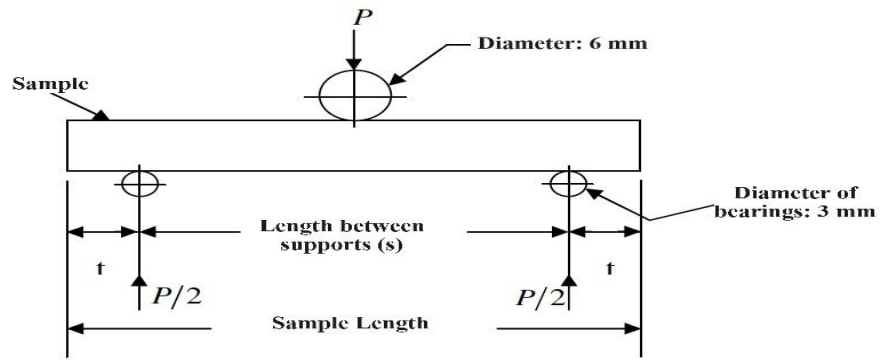


Figure 3.9. Short Beam Shear test setup.

Interlaminar shear strength is the shear stress in vertically loaded, rectangular cross-section beams. It is calculated from the formula as in equation 3.2.

$$S_i = \frac{e P}{4 w \cdot t}$$

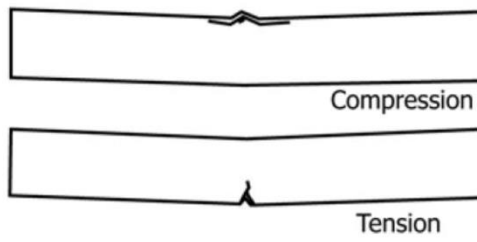
Here, S_i is the interlaminar shear strength, P is the maximum load, w is the width of the sample and t is the thickness of the sample. The samples used in the Short Beam Shear test are very small when $s/t = 4$. Since the diameter of the supports is 3 mm and the diameter of the cylinder load is 6 mm, difficulties are experienced when loading the sample.

Typical damages encountered in the Short Beam Shear test are classified as follows (Figure 3.10).

1. Interlaminar Shear



2. Flexure



3. Inelastic Deformation



Figure 3.10. Typical damages encountered in the Short Beam Shear te

PART 4

RESULTS AND DISCUSSION

4.1 INTRODUCTION

This chapter details the experimental work and explains how the experiments were conducted. Equipment and materials used in this investigation are included. The experimental procedure used to prepare samples accelerated cooling can improve the mechanical properties of the steel. These tests include bending strength, hardness, scanning electron microscope analysis (*SEM*), and the fatigue test.

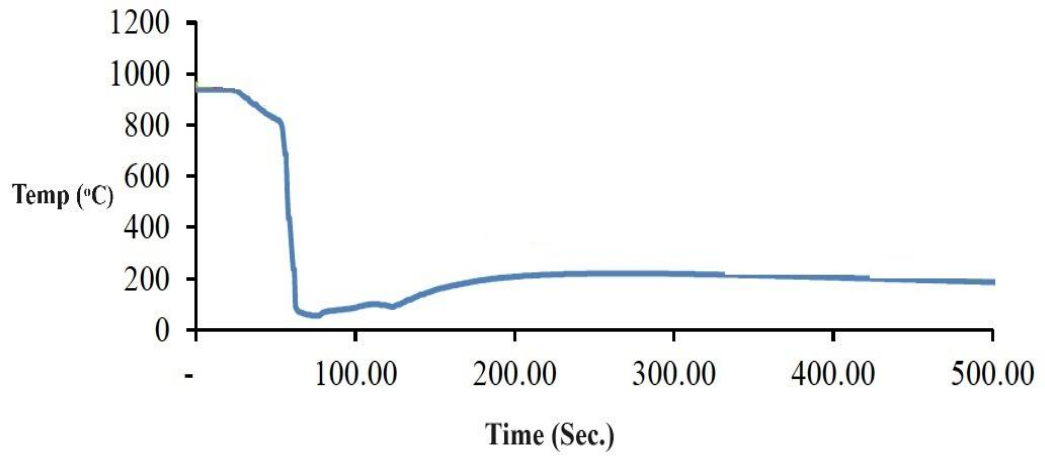
4.2. COOLING RATE

Cooling graphs of web region of profiles subjected to HS-KT heat treatment at different parameters according to time are given in Figures 4.1. When the cooling graphs of the HEA 120 profile on which HS-KT is applied at 2 Layer 12 Bar in Figure 4.1 are examined, it is seen that the cooling graph decreases rapidly from 950°C, which is the austenitizing temperature, due to the application of the HS-KT process to the web region. However, after this rapid cooling on the surface of the profile, it is seen that the temperature values increase due to the effect of the temperature in the core region. Thus, the self-tempering process occurred in the profiles.

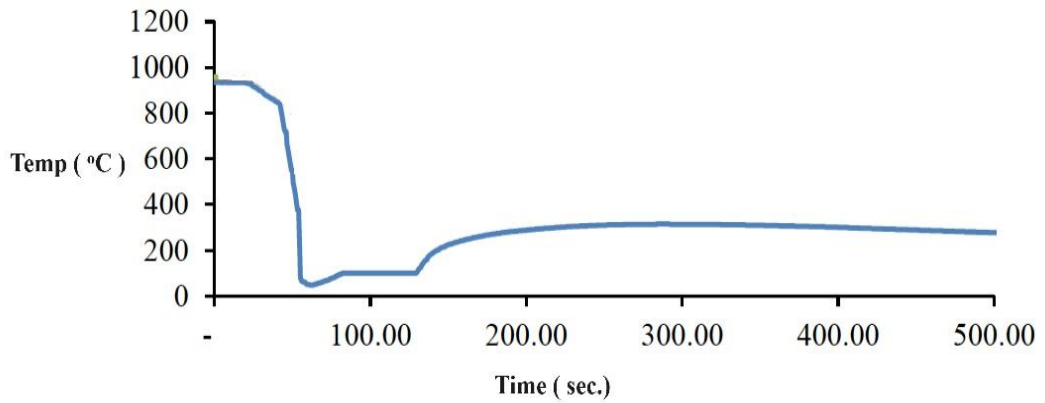
It is observed from the graphs that the cooling rate is lower with the HS-KT heat treatment applied to HEB 120/140 size profiles, which have a thicker cross-section than the HEA 120/140 size profile. Due to the thicker section profile, the self-tempering process either occurred at high temperatures or the end temperature of

cooling was quite high so that there was no need for the self-tempering proces

HEA 120 2 Kat 12 Bar 20 sn.



HEB 120 2 Kat 12 Bar 20 sn.



HEB 140 2 Kat 12 Bar 20 sn.

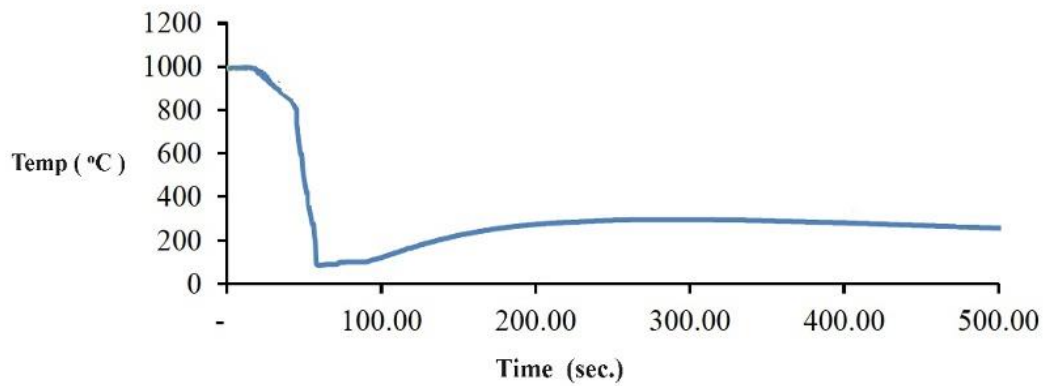


Figure 4.1 Cooling charts.

4.3 BRINELL HARDNESS

The hardness of the examined HEA120 profiles sprayed with air + water at 12 bar pressure are given in Figure 4.2, respectively. While the hardness of HEA120 12 bar HS-KT applied profiles at 2 layers distance increased with the applied time, no difference was observed between the hardness of the web regions under the same conditions. In addition, while the hardness of HEA120 quality profiles with HS-KT applied does not change with the applied pressure, it decreases for 20 seconds at 12 bar pressure. The hardness of HS-KT applied profiles remained slightly low.

The figure shows the Brinell hardness number (HB) measurement results for 3 different steel section types - HEB 120, HEB 140 and HEA 120. The HEB 120 section with height $h=1.5\text{mm}$ showed the highest average hardness of 202.44 HB. This indicates it has the highest resistance to plastic deformation compared to the other sections tested. The HEB 140 section with the largest height of $h=140\text{mm}$ exhibited the lowest average hardness of 155.86 HB. As the height increases, the hardness decreases.

The HEA 120 section with $h=1.52\text{mm}$ showed an intermediate average hardness of 173.89 HB. In general, the hardness tends to decrease with increasing section size/thickness for the S275JR steel alloy. Larger cross sections have lower hardness.

This could be because thicker sections have larger grain sizes resulting from slower cooling during fabrication, leading to softer microstructure. While thinner sections may work harden more.

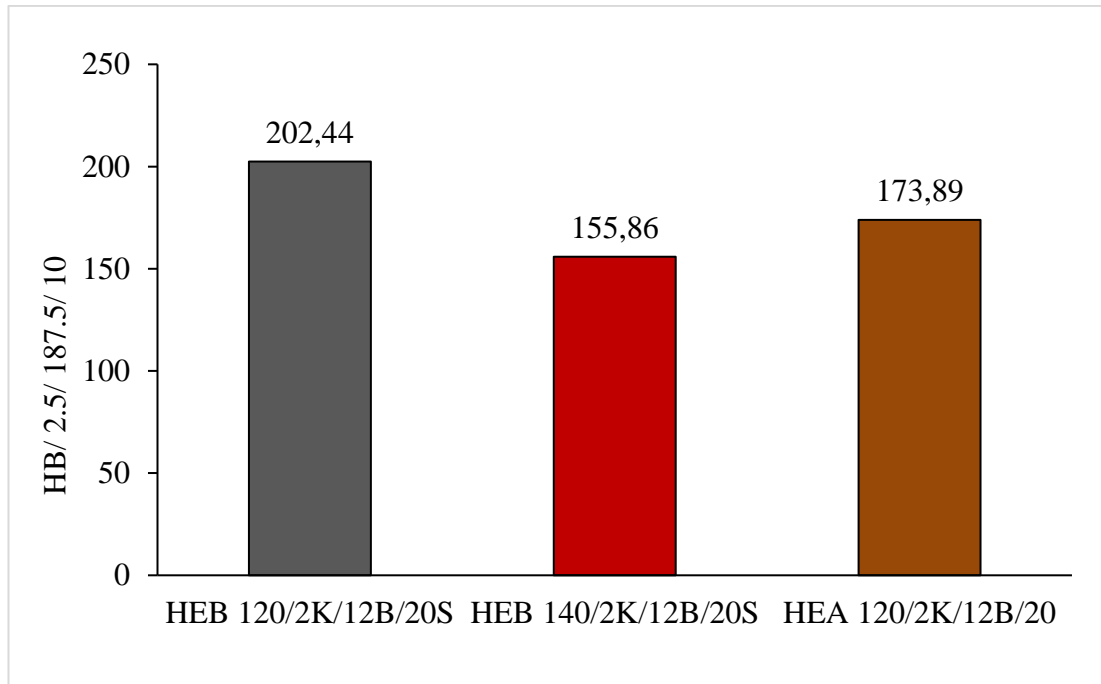


Figure 4.2. Hardness change of the samples.

4.4. BENDING STRENGTH

The provided data shows the flexural strength of different steel samples. Based on the given data, the bending strength of the samples ranges from approximately 339 MPa to 458 MPa. This indicates that the samples have varying resistance to bending forces. The flexural strength values vary for different samples, indicating that the geometry and dimensions of the steel sections (HEB 120, HEB 140, and HEA 120) have an influence on their bending strength. Among the HEB sections, HEB 120 has a higher average bending strength (458 MPa) compared to HEB 140 (343 MPa). The HEA 120 section has the average flexural strength (339 MPa) among the three sections. The differences in flexural strength could be attributed to variations in the composition, microstructure, or heat treatment of the steel samples.

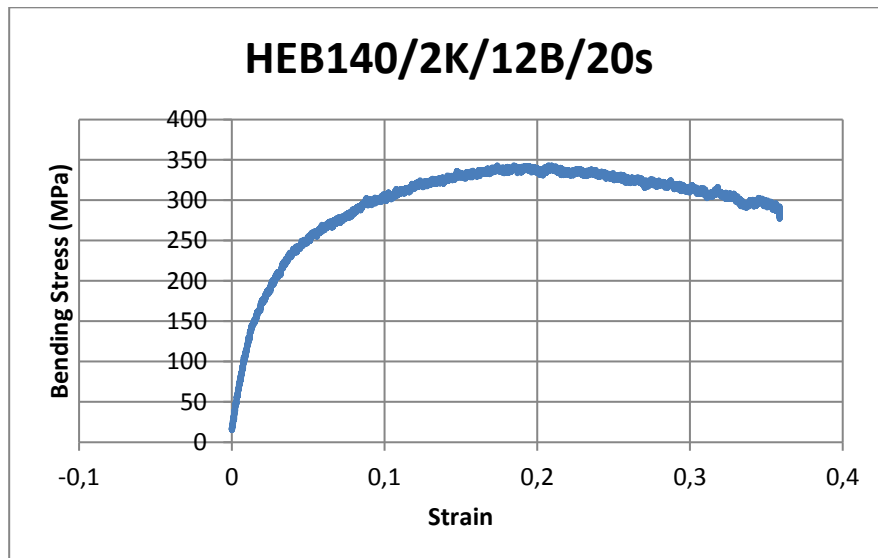
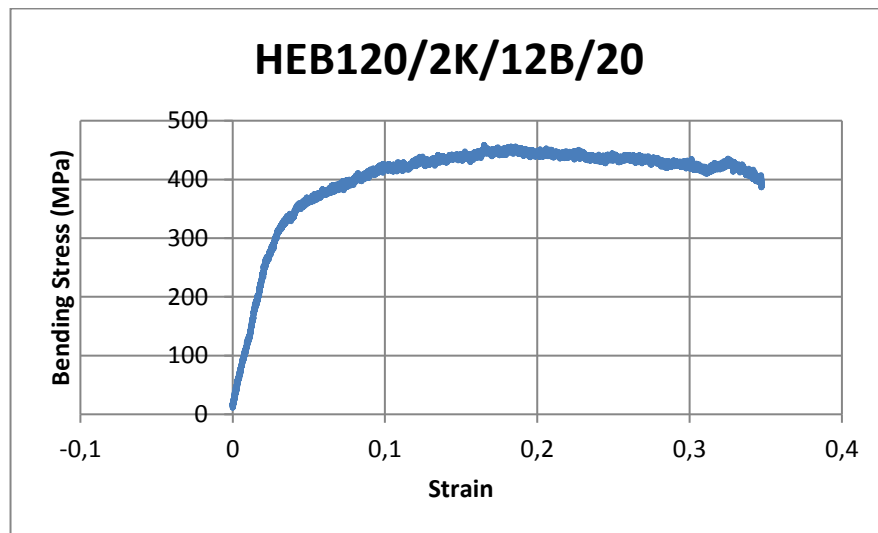
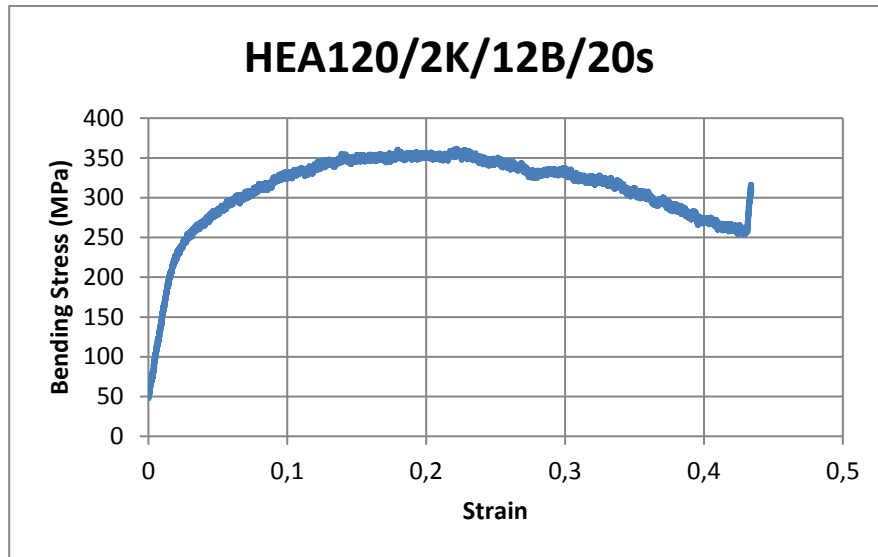


Figure 4.3. Bending stress of the samples.

Table 4.1. Bending stree and maximum bending stress of the samples.

Sample	Bending Yield Strength	Maximum Bending Strength
HEA120/2K/12B/20s	197.5	339
HEB120/2K/12B/20s	250	458
HEB140/2K/12B/20s	145	343

4.5 FATIGUE TESTING

Fatigue testing on steel S275 involves subjecting specimens of the material to cyclic loading conditions to simulate the repetitive stress experienced during its service life. Steel S275 is a low-carbon structural steel with good mechanical properties commonly used in construction and engineering applications. The fatigue test aims to determine how the material's fatigue strength, endurance limit, and fatigue life are affected by cyclic loading. The test involves applying a cyclic load to the specimen, typically in the form of alternating tension and compression, at a constant frequency. The applied stress is usually below the yield strength of the material to avoid plastic deformation.

During the test, the number of cycles to failure (fatigue life) and any changes in mechanical properties such as stiffness and ductility are recorded. This information helps engineers assess the material's performance under repeated loading and design structures with adequate fatigue resistance.

Fatigue tests on steel S275 can be conducted according to various standards such as ASTM E466 or ISO 1099, which provide guidelines for specimen preparation, testing procedures, and data analysis. These tests are essential for ensuring the reliability and safety of structures subjected to cyclic loading, such as bridges, buildings, and machinery components. Figure shown (orange line) represents test data for a HEB 120 12 BAR 2KAT 20SN section with a height $h=1.5\text{mm}$. We can see that as the number of cycles increases, the fatigue strength decreases in a typical S-N curve pattern. The

fatigue limit, which is considered the stress value at 1 million cycles, would be approximately 281 MPa based on extrapolating the data trend.

The green line represents data for the same section profile but with a slightly larger height of $h=1.52\text{mm}$. The fatigue limit based on this data set is estimated to be around 349 MPa, which is higher than for the $h=1.5\text{mm}$ specimen. This indicates that a small increase in thickness can improve the fatigue performance, as there is more material resisting crack initiation and growth. The blue line is for a thicker HEB 140 section. Again following the decreasing stress trend with increasing cycles, the fatigue limit would be around 338 MPa. Steel S275 typically exhibits a fatigue limit or endurance limit, which is the maximum stress amplitude that the material can withstand for a specified number of cycles without failure. This value is often expressed in terms of stress range (σ) or stress ratio ($\sigma_{\text{max}}/\sigma_{\text{min}}$). The fatigue strength of S275 can vary depending on factors such as surface condition, heat treatment, and environmental conditions. In general, S275 has a moderate to high fatigue strength compared to some other structural steels.

Table 4.2. Cooling rates in the web, regions of the samples profile

Sample	web (°C/sec.)	Fatigue value
HEA120 12BAR 2KAT 20SN	77	349
HEB 120 12 BAR 2KAT 20SN	41	281
HEB 140 12 BAR 2KAT 20SN	38	338

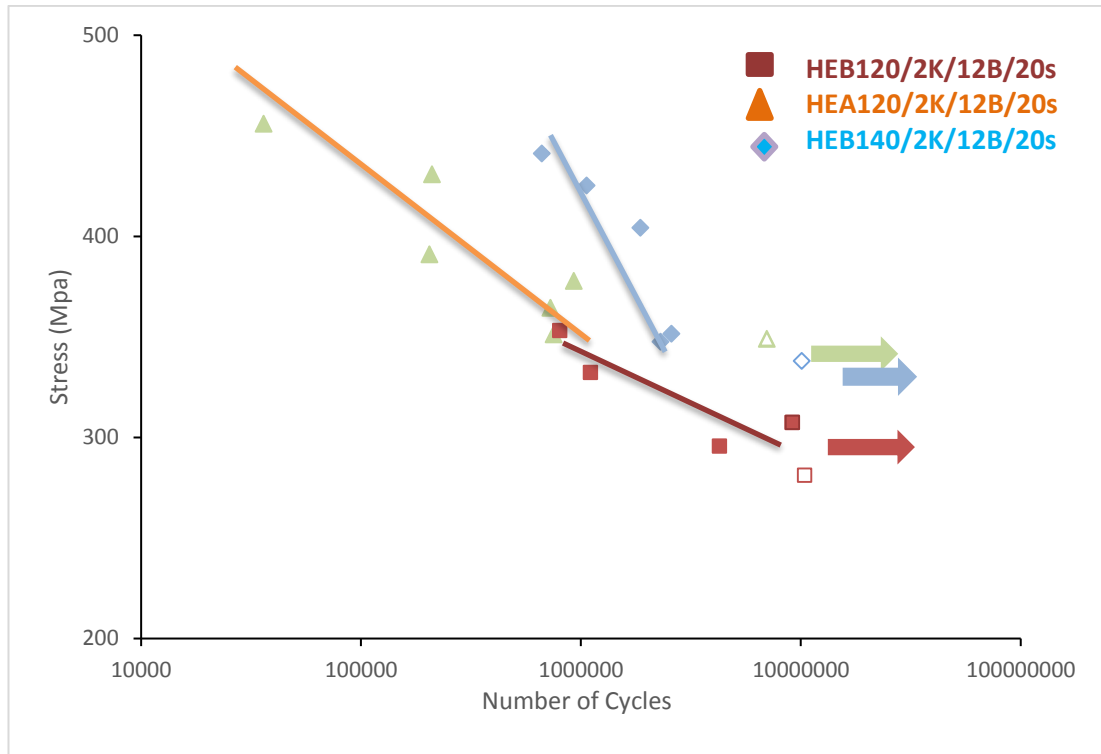


Figure 4.4. Fatigue strength of the samples.

In summary, the fatigue strength decreases with increasing number of cycles for all three specimen geometries, following typical fatigue behavior. The fatigue limit increases slightly with thickness, from 564 MPa for the thinnest section to around 700 MPa for the thicker sections. The reasons why the fatigue limit increases with thickness in steel alloys : Stress concentration effects are reduced, Resistance to crack propagation is higher and Resistance to crack initiation is higher: It takes longer for a crack to initiate from the surface in a thicker section compared to a thin one, as the stressed volume is greater This suggests that material and geometric properties can influence the fatigue performance of S275JR steel, with thicker sections displaying higher resistance to fatigue crack initiation and propagation.

4.6 SEM IMAGES

Due to the large number of samples with different parameters in the thesis study, SEM and EDS studies were limited to HEA 120 size profile and maximum and minimum

quenching parameters. The SEM representation of the web region of the HEA 120 /HEB 12/140 profile to which HS-KT was applied in 2 layer, 12 bar, 20 sec. is given in Figure 4.5- 4.7.. The web provides SEM images and EDX maps of the regions. While Figure 4.6 shows that the examined profile exhibits acicular ferrite and a small amount of bainite microstructure, Figure 4.7 suggests that the examined profile consists of acicular ferrite, bainite and a small amount of martensite structure.

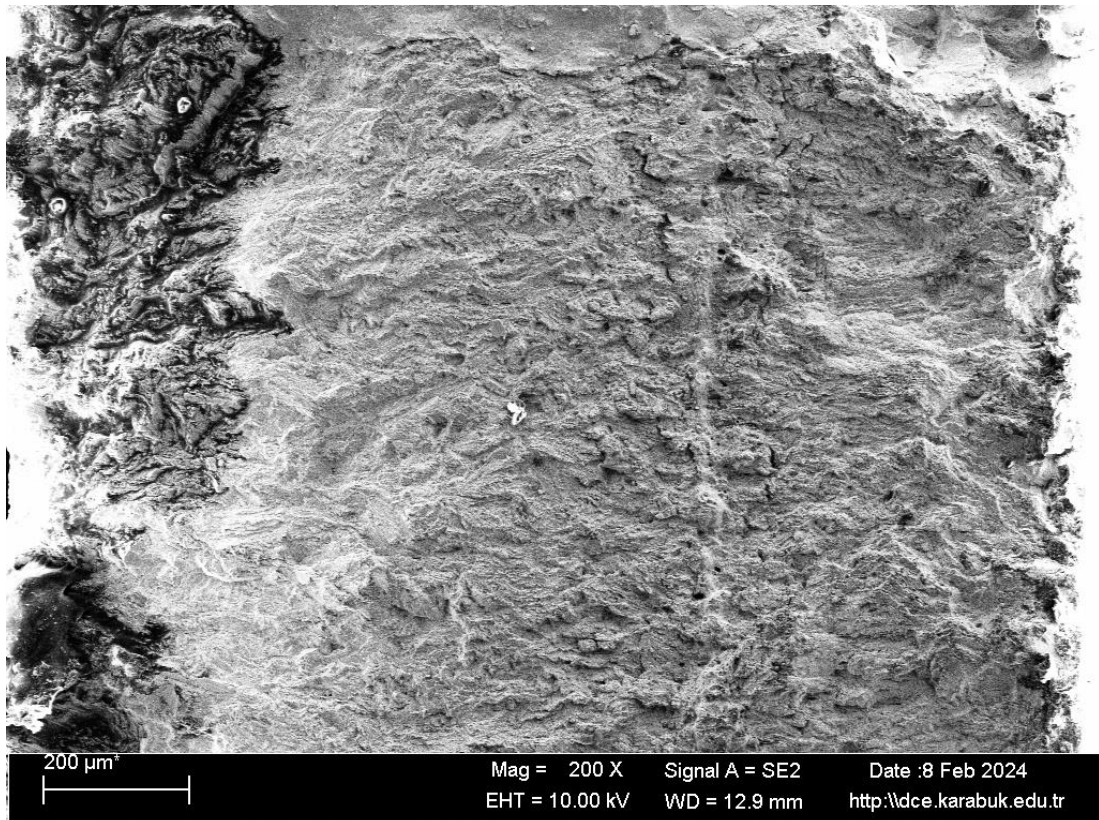


Figure 4.5. SEM of HEA120 quality 12 bar 20 sec. at 200 x SEM image magnification after Fatigue test.

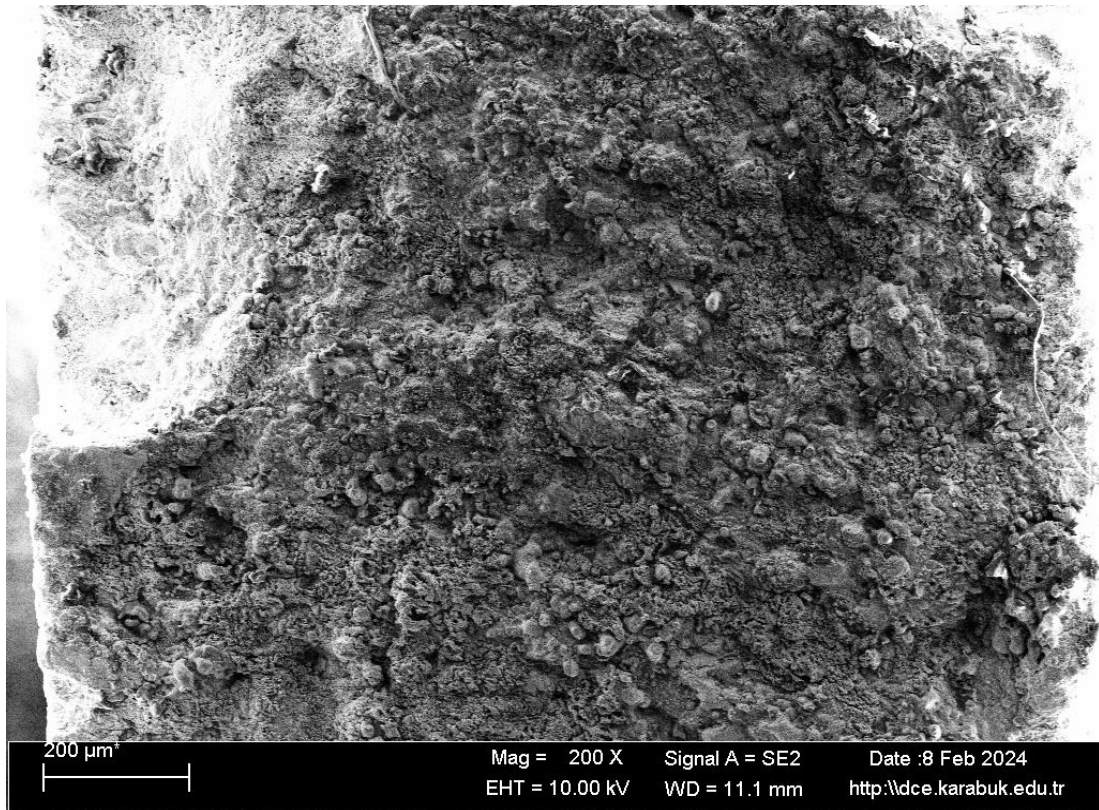


Figure 4.6. SEM of HEB120 quality 12 bar 20 sec. at 200 x SEM image magnification after Fatigue test.

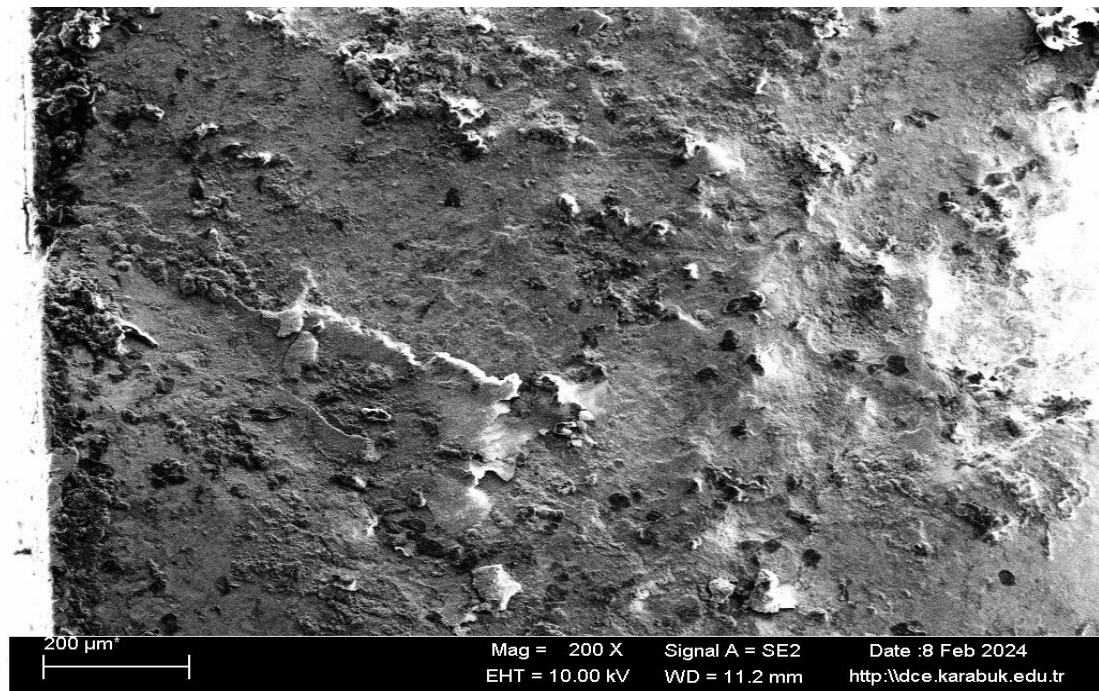


Figure 4.7. SEM of HEB140 quality 12 bar 20 sec. at 200 x SEM image magnification after Fatigue test .

PART 5

CONCLUSIONS

In this study, HS-KT heat treatment was applied to HEA 120 and HEB 120/140 profiles at 12Bar air pressure values of, and cooling times of 20 sec. and 2 coats were applied with different nozzles and different distances between the materials. The results obtained in this study, in which the effect of HS-KT heat treatment on the mechanical properties of H-type steel construction profiles of different sizes was investigated, are listed below;

- i. The fatigue strength decreases with increasing number of cycles for all three specimen geometries, following typical fatigue behavior.
- ii. The fatigue limit increases slightly with thickness, from 564 MPa for the thinnest section to around 700 MPa for the thicker sections.
- iii. Thickness increases the resistance of steel to both crack initiation and propagation mechanisms under cyclic stresses, leading to an improved inherent fatigue limit.
- iv. An inverse relationship between hardness and thickness for the tested S275JR steel sections, with the thinnest HEB 120 displaying the highest hardness. Section size influences the mechanical properties.
- v. The HEA 120 section has the highest average flexural strength, followed by HEB 120 and HEB 140. The specific application and design requirements will dictate the significance of these results in practical use.

REFERENCES

1. DeArdo, A., *Accelerated cooling: a physical metallurgy perspective*, in *Proceedings of the Metallurgical Society of the Canadian Institute of Mining and Metallurgy*. 1988, Elsevier. p. 3-27.
2. Çelik, O., *Nervürlü inşaat çeliklerinin mekanik özelliklerinin incelenmesi*, in *Fen Bilimleri Enstitüsü*. 2015, Karabük Üniversitesi.
3. Özçelik, S., “Mantarı sertleştirilmiş raylarda yorulma davranışı incelenmesi”, (2013).
4. Başkonuş, M. and E. Tekin. “Hızlı Tren Olgusu, Mantarı Sertleştirilmiş ve Beynitli Ray Çelikleri”. in *International Iron and Steel Symposium*. (2012).
5. IŞIKGÜL, A., *FARKLI EBATLARDAKİ H TİPİ ÇELİK KONSTRÜKSİYON PROFİLLERDE HIZLANDIRILMIŞ SOĞUTMA İLE MEKANİK ÖZELLİKLERİN İNCELENMESİ*, in *Metalurji ve Malzeme Mühendisliği Anabilim Dalı*. 2022, Karabük Üniversitesi: Karabük.
6. YAĞIZ, O., *FARKLI HIZLANDIRILMIŞ SOĞUTMA PARAMETRELERİ UYGULANMIŞ PROFİLLERDE KALINTI GERİLİM ÖLÇÜMLERİNİN İNCELENMESİ*, in *Metalurji ve Malzeme Mühendisliği Anabilim Dalı*. 2024, Karabük Üniversitesi: Karabük.
7. YALÇIN, T. and G. ATEŞOK, “Demir cevherlerinin zenginleştirilmesi”, *Scientific Mining Journal*,18(2): 20-32 (1979).
8. TÜRKYILMAZ, S., *ENTEĞRE DEMİR ÇELİK TESİSLERİ YAN ÜRÜNLERİ KULLANILARAK REAKTİVİTESİ ARTTIRILMIŞ KOK ÜRETİMİ*, in *METALURJİ VE MALZEME MÜHENDİSLİĞİ*. 2022, SAKARYA ÜNİVERSİTESİ: SAKARYA.
9. Can, A.Ç., “Tasarımcı mühendisler için malzeme bilgisi”. *Birsen Yayınevi*(2010).

10. Smith, E.H., "Mechanical engineer's reference book". **Butterworth-Heinemann**(2013).
11. Degner, M., "and others. Steel Manual", (2008).
12. Yin, R., "Metallurgical process engineering". **Springer Science & Business Media**(2011).
13. Atgür, M., *Avrupa birliği'ne uyum sürecinde türkiye'de demir çelik sektörü: analizi, sorunlar ve çözüm önerileri*, in *Sosyal Bilimler Enstitüsü*. 2006, Balıkesir Üniversitesi: Balıkesir.
14. Köybaşı, E.H., *İskenderun bölgesindeki demir çelik firmaları özelinde, demir çelik sektörünün ihracatta karşılaştıkları sorunlar ve çözüm önerileri*, in *Sosyal Bilimler Enstitüsü*. 2019, Dokuz Eylül Üniversitesi: İzmir.
15. Bulut, A., *Yapı profillerinde soğutma parametrelerinin ürün özelliklerine etkisinin incelenmesi*, in *Fen Bilimleri Enstitüsü*. 2019, Afyon Kocatepe Üniversitesi: Afyon.
16. Wang, G.C., "The utilization of slag in civil infrastructure construction". **Woodhead Publishing**(2016).
17. PİROĞLU, F., E. UZGİDER, M. VURAL, and Ö.B. ÇAĞLAYAN, "GEÇMİŞTEN BUGÜNE YAPI ÇELİĞİ VE ÖNEMLİ YAPISAL ÖZELLİKLERİ".
18. Yildirim, D., *2205 dubleks paslanmaz çelik ile S355J2 genel yapı çeliğinin birleştirilebilirliğinin incelenmesi*. 2018, Fen Bilimleri Enstitüsü.
19. SHINDE, S. and M. MAY, "RECENT DEVELOPMENTS IN THE USE OF QUENCHED AND SELF-TEMPERED HOT ROLLED H-BEAMS".
20. Rocha, M., E. Brühwiler, and A. Nussbaumer, "Geometrical and material characterization of quenched and self-tempered steel reinforcement bars", **Journal of Materials in Civil Engineering**,28(6): 04016012 (2016).
21. Finnigan, S., B. Charnish, and R. Chmielowski. "Steel and the skyscraper city: A study on the influence of steel on the design of tall buildings". in **CTBUH Conference, New York**. (2015).
22. ZANON, R., G. AXMANN, J.-C. GERARDY, and A. PLUMIER, "The use of heavy rolled sections in High-rise buildings: Current practice and future Innovation".

23. https://sections.arcelormittal.com/repository2/Sections/1_HISTAR_High%20Strength/5_01_24_Histar_ASTM_A913_seismic_ncee_en.pdf.
24. Weber, L., “Histar high performance hot-rolled beams”, (2003).
25. Fujibayashi, A. and K. Omata, “JFE steel's advanced manufacturing technologies for high performance steel plates”, *JFE Technical report*,5: 10-15 (2005).
26. Bo, Z., S. Yong, T. Li, Y. Hong-Xin, C. Wen-Quan, and B. Yao-Zong, “Research on a new process of the non-quenched and tempered steel with high strength and high toughness”, *Physics Procedia*,50: 25-31 (2013).
27. Hoffmann, J. and B. Donnay, “TMCP applications in sections, bars and rails”, *Profilarbed Research*, (2004).
28. Kong, X. and L. Lan, “Optimization of mechanical properties of low carbon bainitic steel using TMCP and accelerated cooling”, *Procedia Engineering*,81: 114-119 (2014).
29. Tang, S., Z. Liu, G. Wang, and R. Misra, “Microstructural evolution and mechanical properties of high strength microalloyed steels: Ultra Fast Cooling (UFC) versus Accelerated Cooling (ACC)”, *Materials science and Engineering: A*,580: 257-265 (2013).
30. Zengin, H., H. Ahlatci, S. Oner, M.E. Demirkazik, S. Ozcelik, Y. Turen, and Y. Sun, “The effect of accelerated cooling on microstructure and impact strength of S355J2 quality steels used in power transmission line construction”, (2018).
31. Snijder, H., L.-G. Cajot, N. Popa, and R. Spoorenberg, “Buckling curves for heavy wide flange steel columns”, *Romanian Journal of Technical Science: Applied Mechanics*,59(1/2): 178-204 (2014).
32. Jung, S.H., M.S. Yun, B.S. Koo, and K.K. Lee. “Influence of Non-Uniform Water Cooling on the Shape of Rolled H-Shaped Beam”. in *HSLA Steels 2015, Microalloying 2015 & Offshore Engineering Steels 2015: Conference Proceedings*. Wiley Online Library (2015).
33. Koo, B.S., “Longitudinal bending behaviors of hot-rolled H-beams by quenching and self-tempering”, *Engineering Failure Analysis*,133: 106009 (2022).
34. Harman, M., *Yüksek mukavemetli çeliklerin farklı kaynak yöntemleri kullanılarak kaynak edilebilirliğinin incelenmesi*, in *Fen Bilimleri Enstitüsü*. 2019, Gazi Üniversitesi: Ankara.

35. Benli, S., “Kaynaklı parçalarda oluşan artık gerilmelerin incelenmesi”, *Yüksek lisans, Dokuz Eylül Üniversitesi Fen Bilimleri Enstitüsü, İzmir*, (2004).
36. YELBAY, H.İ., “TAHRİBATSIZ YÖNTEMLERLE KALINTI GERİLİM ÖLÇÜMÜNDEKİ GELİŞMELER”.

RESUME

Antar ALALIALKHALIL is a material engineer who graduated from the Metallurgy Engineering Engineering, Karabük University - TURKEY. He received his Bachelor's degree in 2021. He is currently studying for his Master's degree at Karabük University in the field of Materials Engineering.